USGS
science for a changing world

Derivation of ground surface and vegetation in a coastal Florida wetland with airborne laser technology

By Ellen A. Raabe, Melanie S. Harris, Ramesh L. Shrestha, and William E. Carter

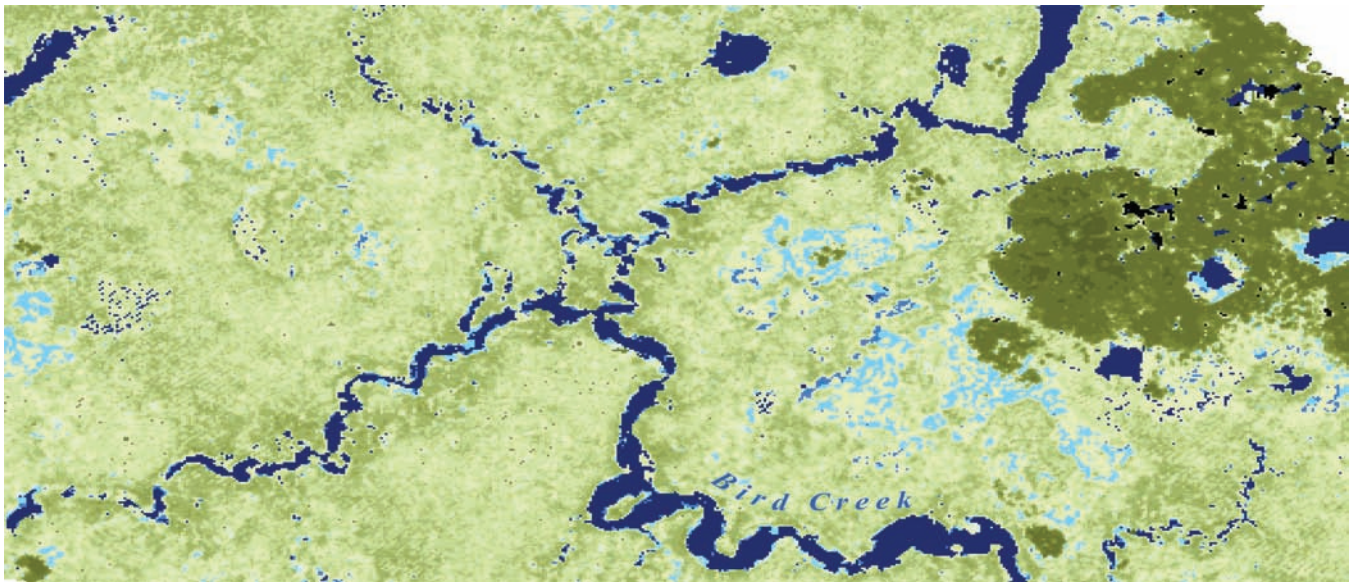

Open-File Report 2008–1125

U.S. Department of the Interior
U.S. Geological Survey

U.S. Department of the Interior
DIRK KEMPTHORNE, Secretary

U.S. Geological Survey
Mark D. Myers, Director

U.S. Geological Survey, Reston, Virginia 2008
Revised and reprinted: 2008

For product and ordering information:
World Wide Web: http://www.usgs.gov/pubprod
Telephone: 1-888-ASK-USGS

For more information on the USGS—the Federal source for science about the Earth,
its natural and living resources, natural hazards, and the environment:
World Wide Web: http://www.usgs.gov
Telephone: 1-888-ASK-USGS

Suggested citation:
Raabe, E.A., Harris, M.S., Shrestha, R.L., and Carter, W.E., 2008, Derivation of ground surface and vegetation in a coastal Florida wetland with airborne laser technology, U.S. Geological Survey, Open-File Report 2008-1125, Saint Petersburg , FL, 41 p.

Contents

Figures

Photos

Tables

Derivation of ground surface and vegetation in a coastal Florida wetland with airborne laser technology

By Ellen A. Raabe, Melanie S. Harris, Ramesh L. Shrestha, and William E. Carter

Abstract

The geomorphology and vegetation of marsh-dominated coastal lowlands were mapped from airborne laser data points collected on the Gulf Coast of Florida near Cedar Key. Surface models were developed using low- and high-point filters to separate ground-surface and vegetation-canopy intercepts. In a non-automated process, the landscape was partitioned into functional landscape units to manage the modeling of key landscape features in discrete processing steps. The final digital ground surface-elevation model offers a faithful representation of topographic relief beneath canopies of tidal marsh and coastal forest. Bare-earth models approximate field-surveyed heights by $\pm$ 0.17 m in the open marsh and $\pm$ 0.22 m under thick marsh or forest canopy. The laser-derived digital surface models effectively delineate surface features of relatively inaccessible coastal habitats with a geographic coverage and vertical detail previously unavailable.

Coastal topographic details include tidal-creek tributaries, levees, modest topographic undulations in the intertidal zone, karst features, silviculture, and relict sand dunes under coastal-forest canopy. A combination of laser-derived ground-surface and canopy-height models and intensity values provided additional mapping capabilities to differentiate between tidal-marsh zones and forest types such as mesic flatwood, hydric hammock, and oak scrub. Additional derived products include fine-scale shoreline and topographic profiles. The derived products demonstrate the capability to identify areas of concern to resource managers and unique components of the coastal system from laser altimetry.

Because the very nature of a wetland system presents difficulties for access and data collection, airborne coverage from remote sensors has become an accepted alternative for monitoring wetland regions. Data acquisition with airborne laser represents a viable option for mapping coastal topography and for evaluating habitats and coastal change on marsh-dominated coasts. Such datasets can be instrumental in effective coastal-resource management.

Introduction

Airborne laser-swath mapping (ALSM) systems collect range data in the form of timed pulse returns from an airborne laser. The two-way travel time (TWTT) of the laser pulse represents an active measurement of the distance from the ground surface to the sensor (Fowler et al., 2001). The laser-ranging vectors can be processed with information from Differential Global Positioning System (DGPS) and aircraft position to derive three-dimensional coordinates (x, y, z values) of each ground position (Shrestha et al., 1999). Objects on the Earth surface, such as buildings and trees, may reflect the laser pulse before it reaches the Earth surface (Kraus and Pfeifer, 1998). A series of post-processing steps is therefore required to extract a bare-earth digital-surface model (DSM) or vegetation characteristics from the cloud of points identified by the laser returns (Axelsson, 1999; Blair et al., 1999; Vosselman, 2000). The acquisition of

distance measurements with an airborne laser altimeter will be referred to as laser altimetry in this report. It is also known as Light Detection and Ranging (LIDAR).

Since the very nature of a wetland presents difficulties for access, navigation, and data collection, airborne coverage from remote sensors has become a widely accepted alternative for monitoring wetland regions. Extensive work has been conducted in wetlands using aerial photography, satellite imagery, and airborne sensors, but the earlier body of work focuses on classification and change detection using spectral reflectance of the vegetation and land surface (Lee and Lunetta, 1995; Raabe and Stumpf, 1997). An essential but missing component is an accurate representation of the surface topography that dictates submergence, exposure, salinity, and habitats in coastal lowlands (Lyon and McCarthy, 1995; Mitsch and Gosselink, 2000).

Wetlands are responsive to minor differences in surface-drainage network, flooding regime, topography, and sediment movement (Stoddard et al., 1989; Montague and Odum, 1997; Day et al., 1998). Currently available digital elevation along the marsh-dominated Gulf Coast of Florida has a horizontal resolution of 30 m and vertical resolution of 1.5 m, or 5 ft (USGS, 2007). This level of topographic detail is inadequate for understanding tidal processes in a coastal region, where elevation differences of centimeters to decimeters correspond to distinct tidal-flood zones and habitats (Clewell, 1997; Stumpf and Haines, 1998; Williams et al., 1999). Morphological characteristics for hydrodynamic modeling have been derived from airborne laser data (Gomes Pereira and Wicherson, 1999; Sallenger et al., 2003), but Baltsavias (1999) argued that the geomorphology derived from most laser-altimetry processing algorithms is 'non-intelligent' and eliminates important topographic features.

Extraction of the ground surface to $\pm$ 0.10 m under vegetation canopy has been achieved in some studies but required extensive mathematical modeling of the surface (Kraus and Pfeifer, 1998; Ackerman, 1999). A 10-m grid has been used to determine the ground surface under a tree canopy but without field verification (Means et al., 2000). The typical vegetation cover of tidal marshes of Florida's Gulf Coast is 0.3 to 1.4 m tall (Clewell, 1997). Earlier laser-altimetry data on this marsh coast presented vertical errors on the order of $\pm$ 0.40 m, attributable to laser-pulse detection errors and thick vegetation (Carter et al., 1999). Test flights with improved calibration methods over a bare road surface produced a vertical accuracy of $\pm$ 0.10 m or better (Shrestha et al., 1999).

Knowing the instrument accuracy that was achievable over a non-vegetated surface, a method was developed to derive a representation of ground surface in the coastal marsh and forest with more detail than the currently available digital models (Iavarone, 2002). In this non-automated approach, the coastal region was partitioned into unique landscape elements, and each element was processed separately. Low- and high-point filters were used to extract ground-intercept and vegetation-intercept data points for bare-earth and vegetation-canopy surface models. Filter search space was adjusted to determine the optimal balance between generalizing elevation under canopy and preservation of topographic detail. We compared ground-surface DSM derived from 2-, 5-, and 10-m filters to field-collected orthometric heights (O.H.) NAVD88.

This report covers several objectives:

- to separate ground-surface intercepts from vegetation intercepts for each landscape element,
- to model the ground surface from laser-derived O.H. to within $\pm$ 0.2 m of ground-control O.H. with a horizontal resolution of 20 m or less,
- to model the vegetation canopy across marsh and coastal forest,
- to derive profiles, shoreline, habitat, and land-cover parameters.

Study Area

Tidal marshes stretch virtually unbroken along Florida's Big Bend coast (Fig. 1). The coastal landscape is a mosaic of tidal creeks, tidal marsh, elevated coastal hammocks, and coastal forest inland of the marsh (Raabe and Stumpf, 1997). Underlying karst limestone is near surface or exposed, and the Floridan aquifer flows through seeps and springs into the tidal marshes (Rupert and Arthur, 1997; Raabe and Bialkowska-Jelinska, 2007). Relict sand deposits provide occasional relief in the coastal lowlands, and

surface features reflect underlying limestone-fracture patterns at some locations (Hine et al., 1988; Vernon, 1951). The tide range is 1 m, and local topographic gradients are 1:1000 or less (Clewell, 1997; Raabe and Stumpf, 1997). Narrow elevation ranges of less than 0.5 m separate tidal submerged, emergent, and upland habitats (Clewell, 1997; Williams et al., 1999). Coastal-forest morbidity and expansion of the tidal marsh inland have been attributed to the relatively flat terrain and recent sea-level rise on this coast (Raabe et al., 2004; Stumpf and Haines, 1998; Williams et al., 1999).

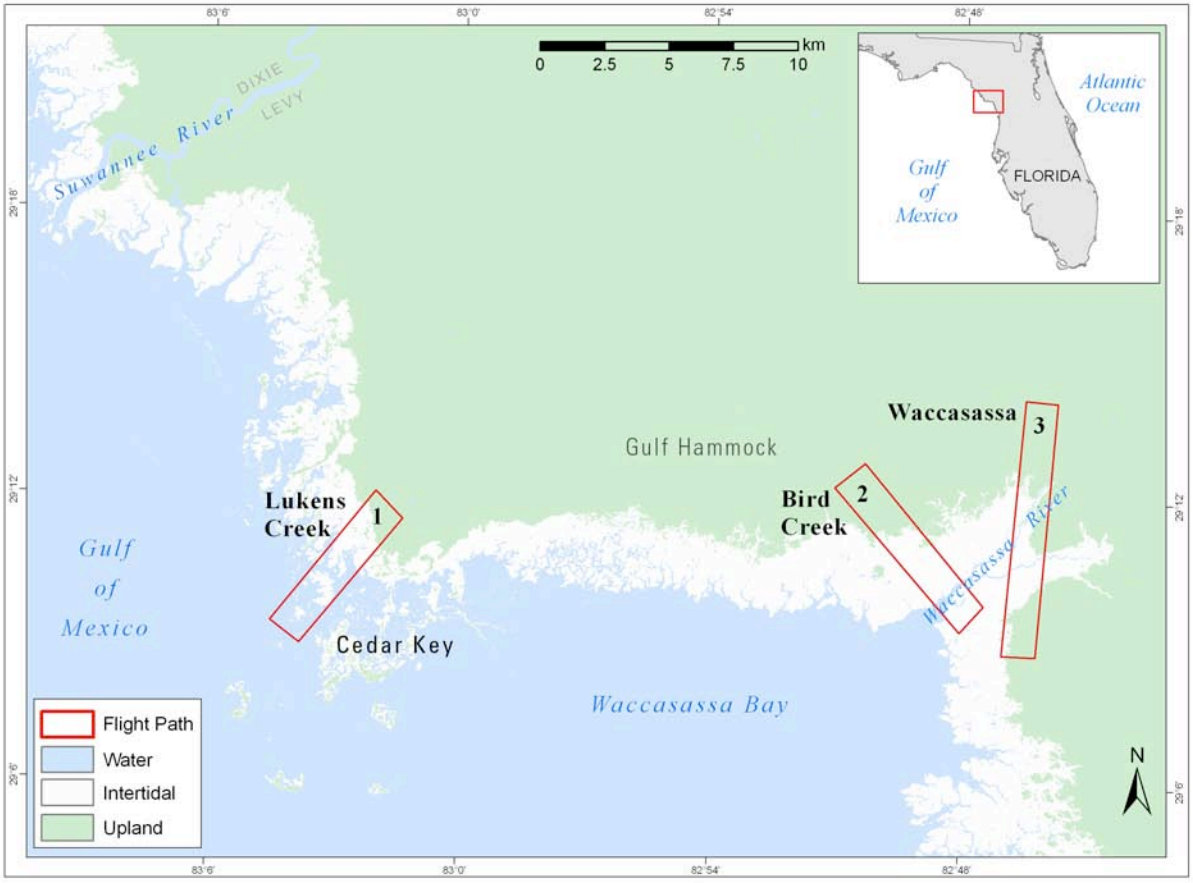

Figure 1. Locations of airborne laser-altimetry flights at Lukens Creek, Bird Creek, and Waccasassa, August, 17, 1999.

Airborne laser flights were undertaken in Levy County, Florida, near Cedar Key and Waccasassa River (Fig. 1). Flight paths included Lukens Creek (1), Bird Creek (2) and Waccasassa (3). Site 1 was selected for shallow tidal creeks, extensive low marsh, a recent burn, and relict sand dunes in the adjoining uplands (Photo 1). Site 2 was selected as representative of a deep, spring-fed tidal creek, near-surface limestone, and a thick cover of the high marsh, black needlerush, *Juncus romerianus* (Photo 2). Site 3 was selected to cover the transition zone between tidal marsh and coastal forest along the Waccasassa River (Photo 3). The sites lie within the Cedar Key Scrub State Reserve and the Waccasassa Bay State Preserve and were accessed via boat, airboat, and dirt road to obtain field-based ground elevations and reconnaissance.

Photo 1. Low marsh at Site 1, Lukens Creek.

Photo 2. Black needlerush at Site 2, Bird Creek.

Photo 3. Coastal forest at Site 3, Waccasassa River.

Methods

Ground Control

Field surveys with DGPS and geodimeter were conducted in the salt marsh and adjoining forest to collect ground-control elevation measurements. Sites were selected to represent elevations from tidal wetlands to elevated uplands and from sparsely vegetated to thick-canopied habitats. DGPS data were collected with a roving kinematic antenna and a stationary base station linked to local vertical control (Raabe et al., 1996). The DGPS antennas were mounted on 2-m poles for unobstructed data acquisition above marsh vegetation (Photo 4). The geodimeter was employed to survey a closed-level loop from DGPS ground control in the open marsh to ground-control sites in the closed-canopy forest (Photo 5). Eighty-five horizontal, x, y-value (UTM 17R NAD83) and vertical, z-value (NAVD88) ground measurements were collected. Four positions were reoccupied for redundancy (Table 1). Position 001 was re-occupied twice. Overall DGPS survey vertical accuracy was 0.008 $\pm$ 0.005 m. Surveyed field elevations ranged from 0.28 to 1.7 m NAVD88. Vertical ground control was used to evaluate and to select an effective method for deriving a ground-surface model in a vegetated environment from laser altimetry (Appendix I).

Table 1. Redundancy in DGPS ground survey.

Position	Northing Difference (m)	Easting Difference (m)	Vertical Difference (m)
001	0.000	0.000	0.0170
012	0.002	0.111	0.0010
023	0.097	-0.020	0.0130
037	0.000	0.001	0.0330
Mean/Std	0.02/0.04	0.018/0.05	0.019/0.014

Photo 4 Differential GPS roving antenna in high marsh at Lukens Creek.

Photo 5. Roving antenna and geodimeter in black-needlerush marsh.

ALSM Data Acquisition and Processing

ALSM data were collected at three pre-specified locations on August 17, 1999 (Fig. 1). Tide range for the day was –0.312 to 0.550 m, and the timing of the flights coincided with the lowest tides of the day in an effort to capture the details of the tidal-marsh-drainage network (Table 2). First and last return with intensity were recorded for each pulse. Base stations, part of a previously established DGPS vertical

network (Raabe et al., 1996), were occupied near Cedar Key and Waccasassa River. Accuracy, precision, and calibration of laser-instrument measurements are discussed by Shrestha et al. (1999).

Laser-altimetry data were processed with proprietary software from Operational Technologies Corporation (Carter et al., 1999). Horizontal coordinates (x,y) were converted to Universal Transverse Mercator (UTM) 17R NAD83. Vector lengths were converted to elevation (z values) as NAVD88 orthometric heights (O.H.). Intensities (I) for each laser pulse were recorded and included in the dataset.

Table 2. Data collection and technical specifications.

Data Collection	Technical Specifications	ALSM Specifications
August 17, 1999	ALTM Model 1210, Optech Inc.	10kHz pulse repetition rate
11:30 am to 2:10 pm	Mounted on Cessna 337	12 Hz scan rate
Lukens Creek (6 km^2)	Ashtech GPS and Aplanix INS	+/-19 degree scan angle
Bird Creek (4 km^2)	Class IV Laser	500 m flying altitude
Waccasassa (4.5 km^2)	1064 nm Laser wavelength	60 m/s average speed over ground
Tide level -0.312 to -0.024 m MSL	10,000 pulse per second	344 m swath width; 65% overlap
2 DGPS Base Stations	Single return & intensity	30 cm diameter footprint

Digital-Surface Model

A bare-earth Digital-Surface Model (DSM) was developed in phases. Flight paths were pieced together to create a mosaic for each site. The team developed an interactive filter program to extract lowest or highest points (z values) from each mosaic with adjustable parameters specified by the analyst. Parameters included filter cell size, number of lowest or highest points per cell, and the option of defining an elevation minimum and/or maximum. Definition of a lower and upper limit for each pass allowed the analyst to develop layers representing functionally different portions of the landscape and to separate ground intercepts from vegetation intercepts.

The choice of planar-grid spacing from fine (1 m) to coarse (20 m) in post-processing was fundamental to retaining detail where possible while modeling actual ground surface under vegetation canopy. Where true ground returns were closely spaced, fine-cell spacing could be used to model the ground surface without interference from vegetation canopy. Where suitable ground returns were sparsely distributed, a coarse-cell spacing optimized extraction of true ground returns and minimized interference from vegetation intercepts. By partitioning the landscape into functional units, the analyst could retain details of topographic features without modeling vegetation artifacts under thick canopy.

An initial surface was created with ordinary kriging to interpolate low-point-filter (LPF) results to a 1-m grid. Preliminary break points for landscape elements were identified in the z-value histogram and corroborated with field measurements of O.H. and vegetation height from previous elevation surveys (Raabe et al., 1996; Raabe et al., 2000; Williams et al., 1999).

Break points for three zones were established, and a mask was created for each layer. Data points below -0.5 m were determined to be in error and were eliminated by setting –0.5 as the minimum elevation. Z values between -0.5 and 0.2 m represent the un-vegetated and submerged portions of tidal creeks, tributaries, and water bodies. The first mask was created to partition this tidal-drainage portion of the landscape. The initial 1-m DSM under this mask was retained to preserve maximum detail of tidal-creek morphology.

The second mask was derived from a 2-m high-point-filter (HPF) where z values exceeded 1.9 m. This mask separated elevated ground and thickly forested areas from low-elevation features, marsh, and single-storied scrub habitat. The final mask was created to include landscape elements with elevations greater than 0.2 m and excluded from the 1.9-m HPF partition. This third partition included tidal marsh, grassland, and scrubland along the coast. An example of a data cloud and the three landscape partitions are shown in Figure 2.

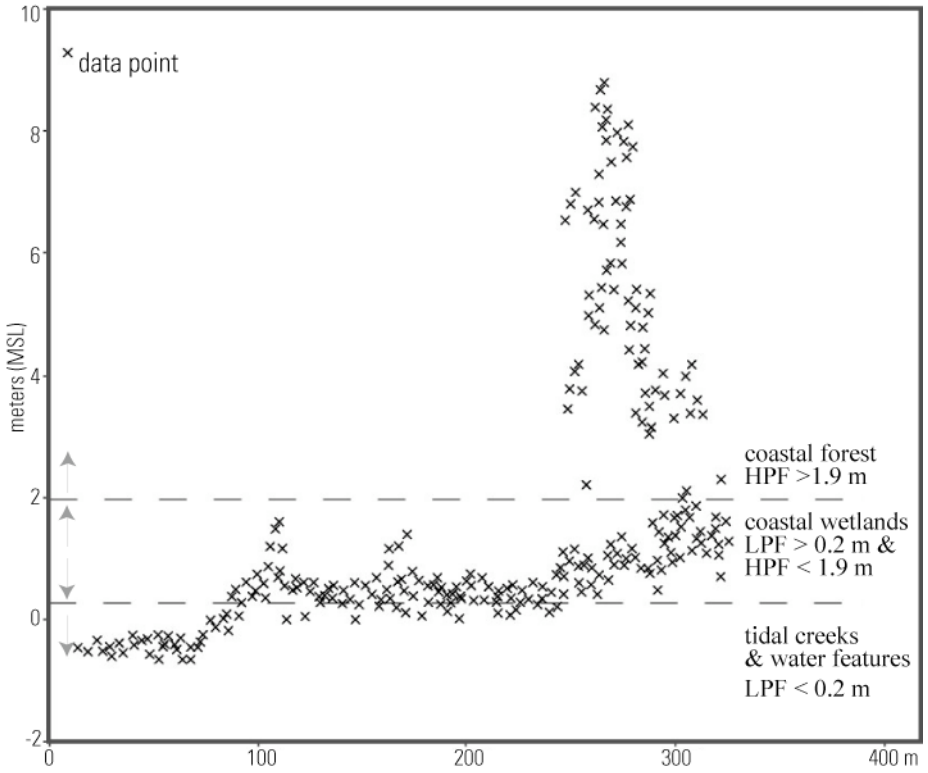

Figure 2. Example data cloud and break points for functional landscape units.

Subsequent surface models for each zone were derived from LPF series and evaluated against field-surveyed ground control. Parameters were varied one at a time to facilitate comparisons between interpolated surfaces and ground-control O.H. Filter cell size was varied sequentially to isolate laser-pulse returns that fully penetrated the vegetation, while maintaining as much detail of the topography as possible. Low-point filters of 2, 5, and 10 m were applied iteratively to each set of data points. Only one point per cell was selected for each 2-m pass. One, three, and five points per cell were selected and averaged for each 5- and 10-m pass. Local topographic charts show no elevation in the area exceeded 4.6 m (15 ft). A corresponding ceiling of 5 m was set in the LPF extraction process.

Results of each iteration of the LPF were interpolated to a 2-m grid using point kriging and a search ellipse of 15 (2 and 5 m) or 30 m (10 m). A surface was created by interpolating between the data points and by re-combining the layers to create a single elevation model. A comparison was made between modeled z values and corresponding field-survey elevations. The absolute difference between each set of points was calculated and summary statistics on the differences were obtained.

Results

Bare-earth and canopy-height models, land-cover categories, shoreline, and topographic profiles were derived from the laser-altimetry data. The development and selection of a bare-earth or ground-surface DSM was based on a "best-fit" approach to minimize differences between modeled z values and field-survey O.H. The data were further explored for the potential of identifying land-cover categories, geomorphology from profiles, and shoreline.

Bare-Earth DSM

Z values in the laser-acquired ground-surface DSM were compared with field-collected O.H. to assess correspondence of the DSM to ground-control elevations (Fig. 3). The 2-m LPF provides the "best-fit" model for the marsh ground surface at Lukens Creek with a correspondence of 0.11 $\pm$ 0.06 m (Fig. 3a).

This filter resolution retains considerable detail of the marsh surface with little interference from vegetation intercepts. The variability in standard deviation is attributable to three factors: 1) the variability of true surface elevation within a 2-m plot, 2) the limited probability that a field-surveyed point corresponds precisely to the laser-ground intercept, and 3) interpolation and model artifacts.

In thickly vegetated areas, the coarser 10-m filter achieved a 0.14 $\pm$ 0.08-m correspondence with field-surveyed O.H. (Fig. 3b). The 10-m filter provided the "best-fit" ground-surface model under forest canopy at all sites, and thick marsh grasses at Bird Creek and Waccasassa. LPF extractions at 2 m and 5 m retained too many vegetation intercepts to represent the ground surface accurately. The DSM from the 10-m LPF retains the general topographic elements of the landscape. Although it lacks the detail obtained in the marsh at Lukens Creek, the model is an improvement over existing surface models (USGS, 2007).

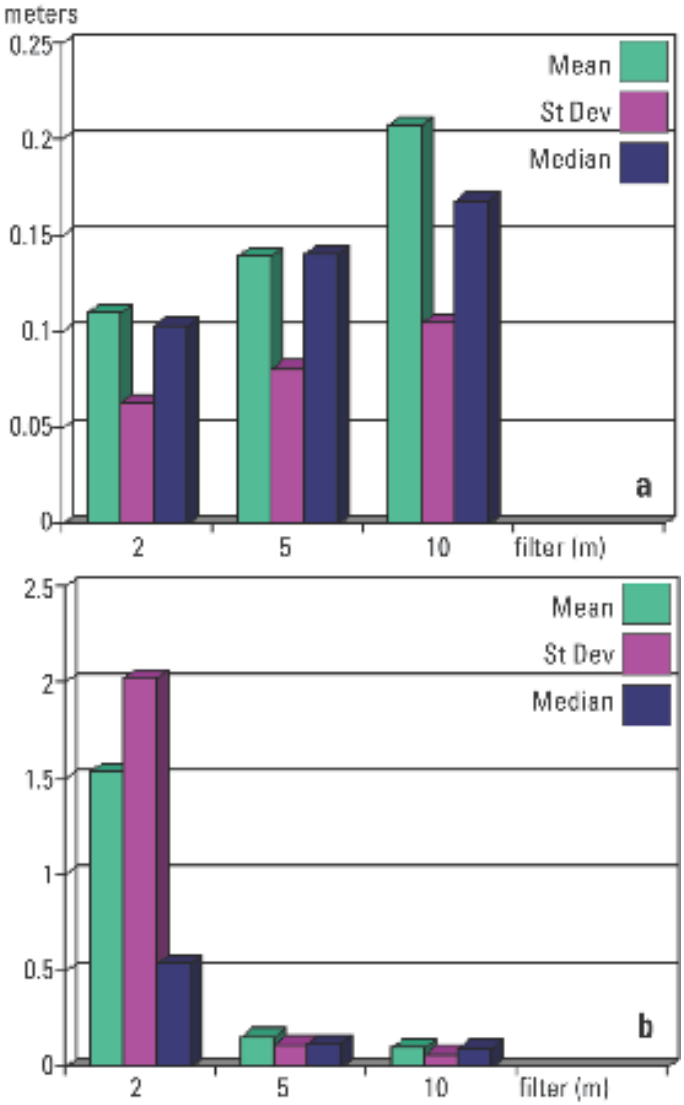

Figure 3a, b. Differences between field-surveyed and surface-model elevations using 2-, 5-, and 10-m filters for a) marsh at Lukens Creek, b) forest and thick marsh.

Final model results were based on filters using one data point per filter cell. Filtered points were interpolated and combined in a 2-m grid to create a final DSM. Three grids, tidal creeks, marsh, and forest, were combined into one DSM for each area, showing details of tidal creeks, marsh-surface features, and the topography beneath the forest (Figs. 4, 5).

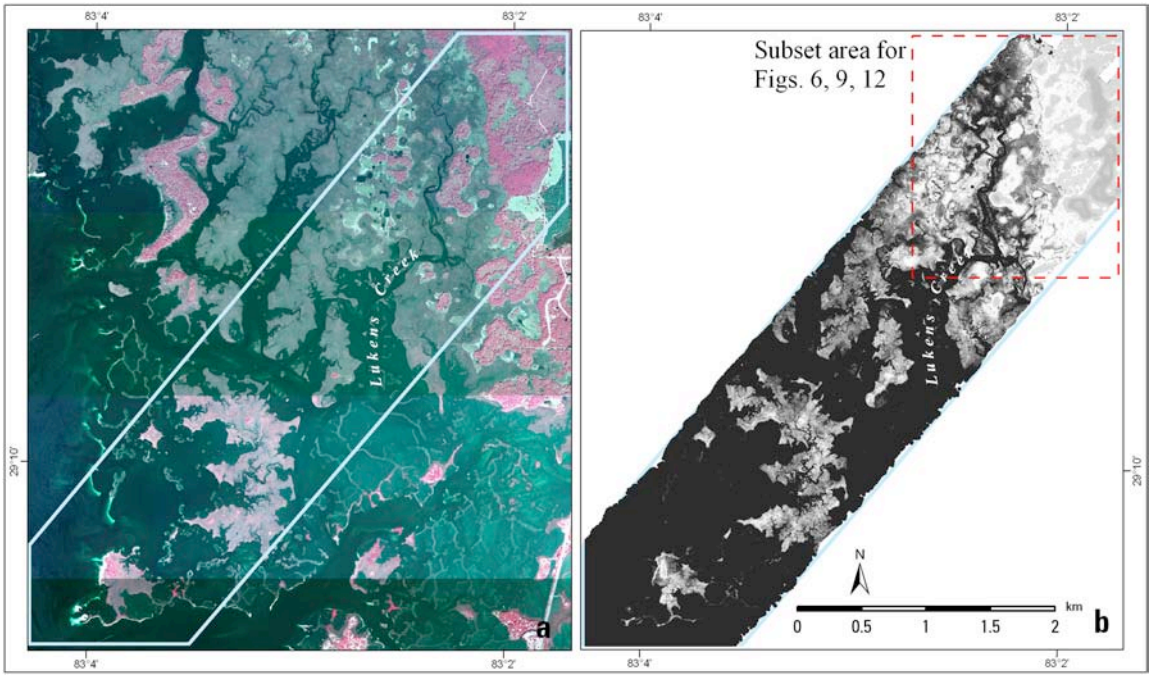

Figure 4. (a) Orthophotoquad, and (b) ground-surface DSM at Lukens Creek.

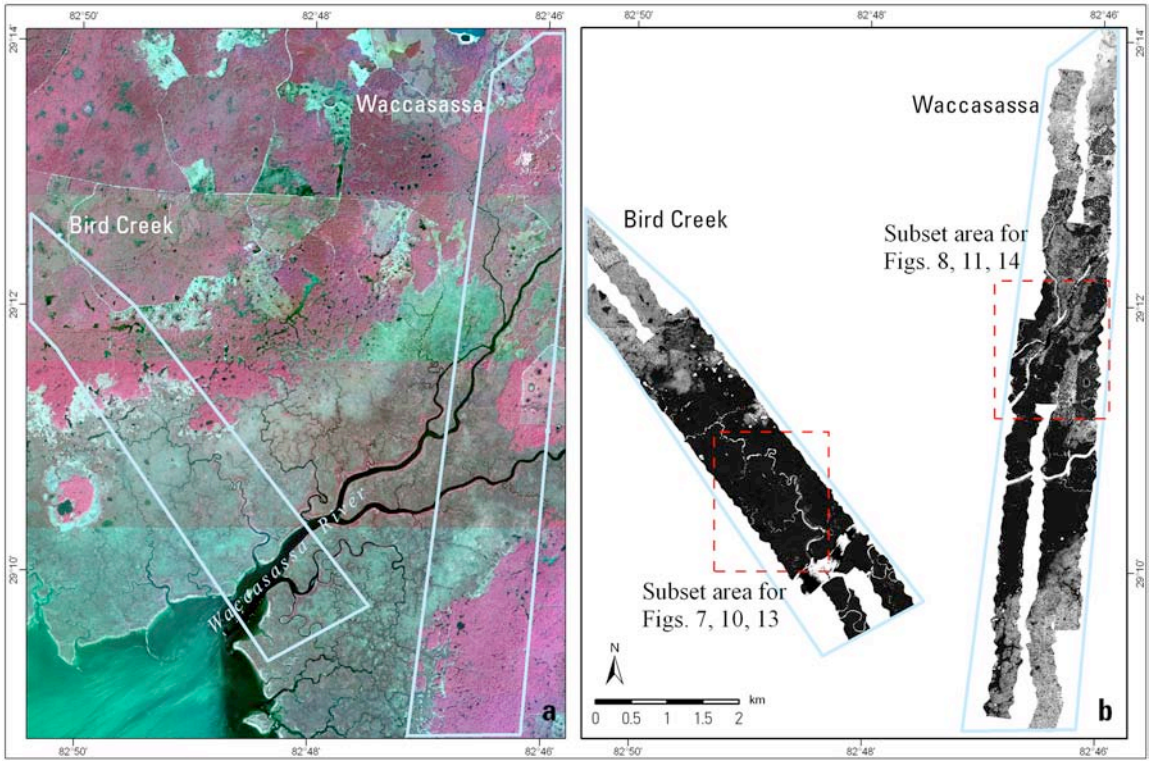

Figure 5. (a) Orthophotoquad, and (b) ground-surface DSM at Bird Creek and Waccasassa.

Color-coded versions of ground-surface DSM are shown in Figures 6, 7, and 8. The majority of tidal marsh occurs at elevations of 0.2 to 0.6 m. The transition from tidal marsh to forest begins at approximately 0.6 to 0.7 m (Photo 6). Morbid forested areas show as individual spikes scattered across the interior tidal marsh in the surface model (Fig. 6 and Photo 7). Where trees are still alive, soil and root

mounds, approximately 0.5 m high, contrast with the surrounding lowered land surface (Raabe et al., 2007; Raabe et al., 2004). Forest floor below ~0.9 m indicates low-elevation swamp areas susceptible to flooding and storm-surge influence. Relict sand dunes at Lukens Creek occupy the 1.7 to 4.6-m range (Fig. 6). Elevations in the Bird Creek and Waccasassa area do not exceed 1.6 m (Figs. 7, 8). Other important features include high levees along Bird Creek and Waccasassa River (Photo 8), silviculture activities, karst-controlled tidal creeks, and sinkholes (Photo 9). An August acquisition date resulted in intercepts with thick canopy forest and interfered with ground intercepts. Artifacts of the LPF process and intercepts with thick forest canopies are indicated in the forested areas as no data.

Photo 6. Transition from tidal marsh to forest at Bird Creek.

Photo 7. Morbid forest with standing dead Sabal palms at Lukens Creek.

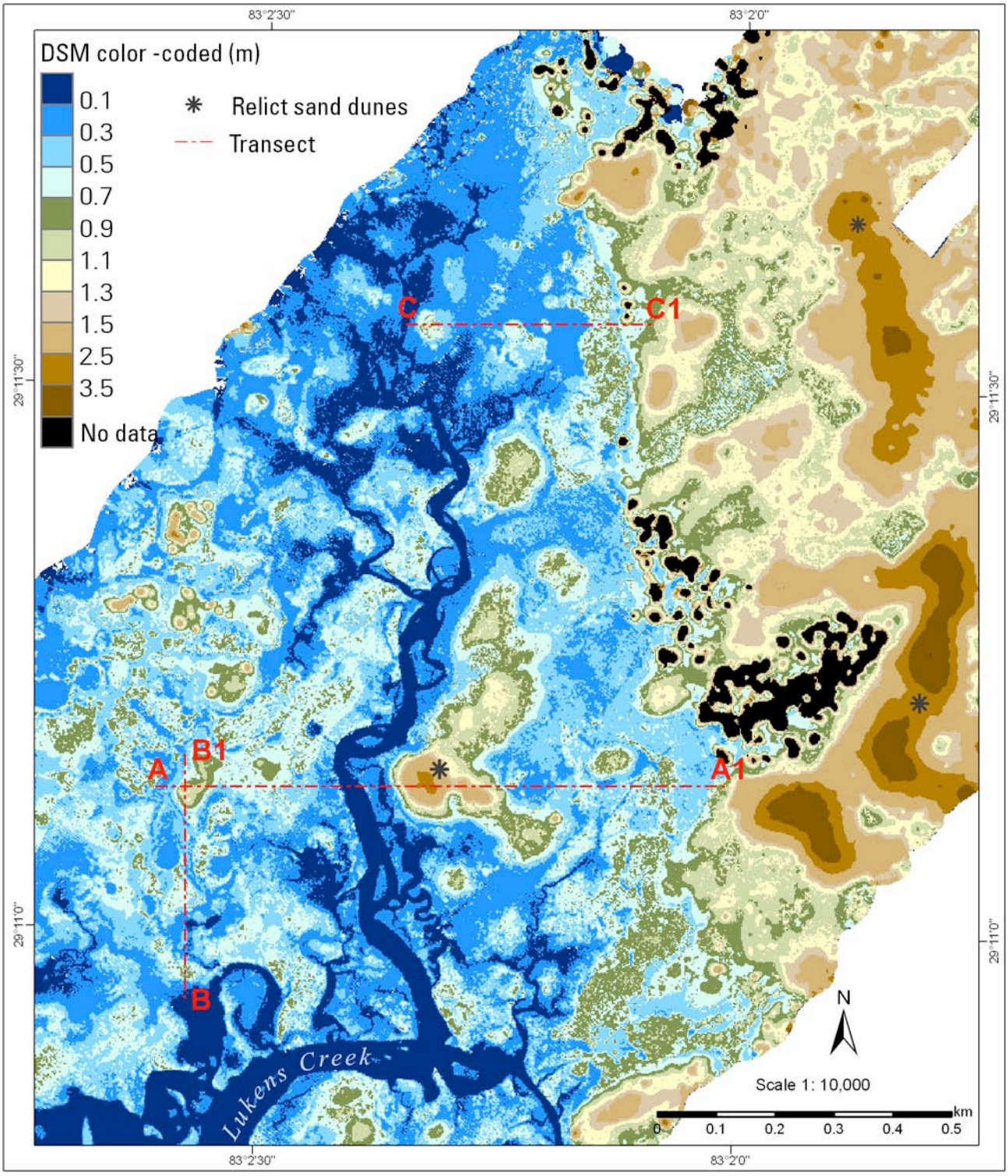

Figure 6. Bare-earth digital-surface model at Lukens Creek derived from ALSM.

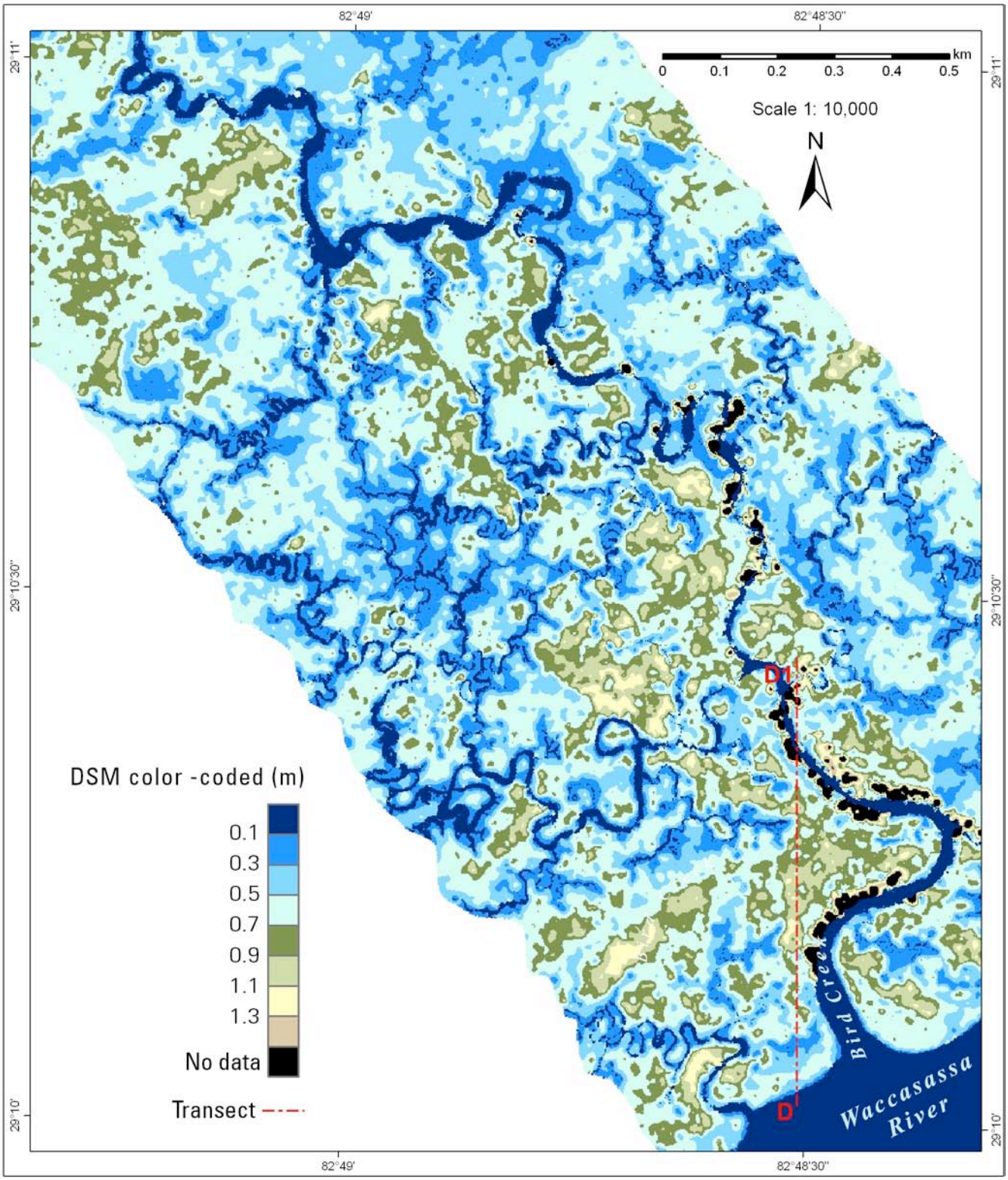

Figure 7. Bare-earth digital-surface model at Bird Creek derived from ALSM.

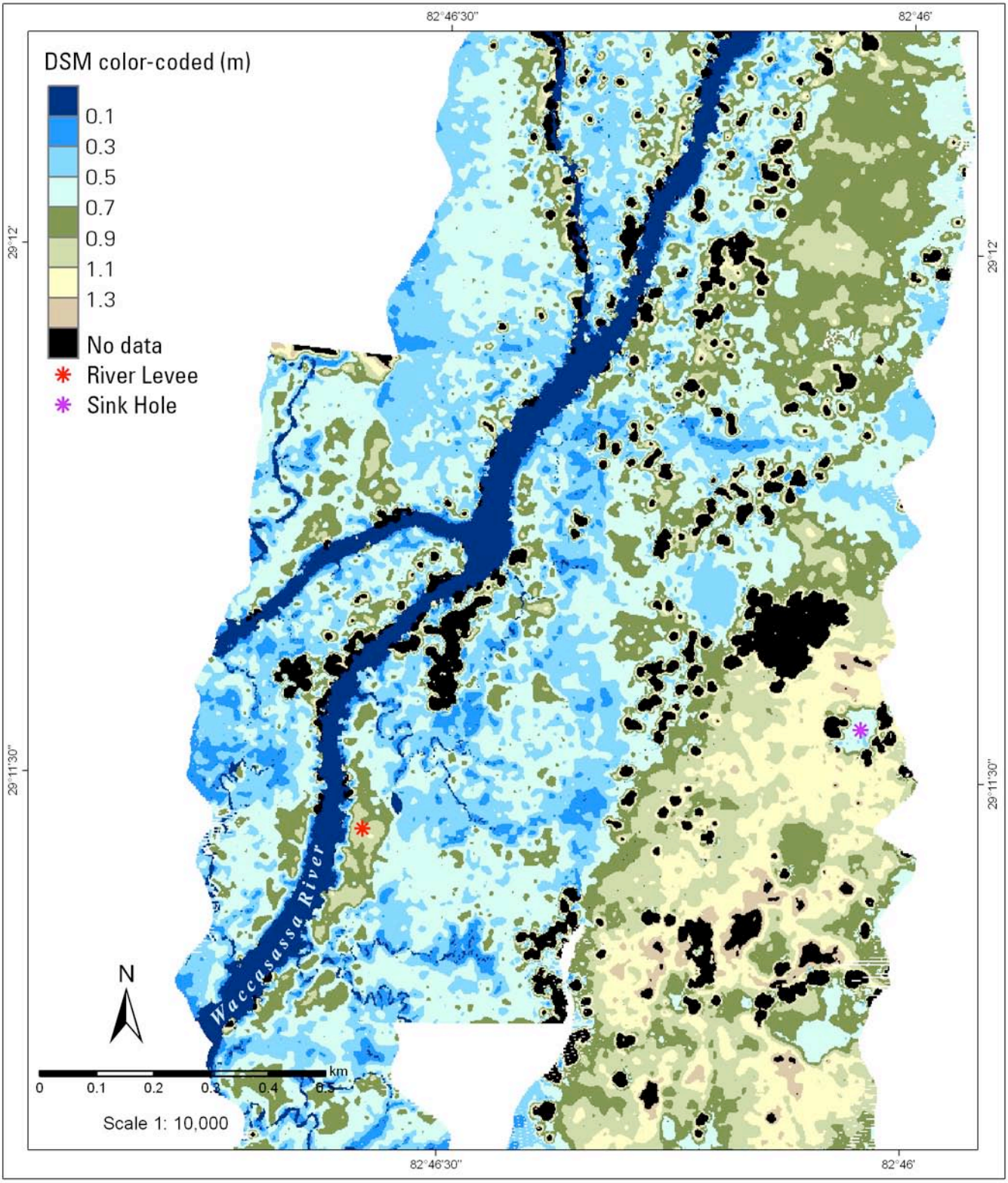

Figure 8. Bare-earth digital-surface model at Waccasassa River derived from ALSM.

Photo 8. Bird Creek levee with scrub and coastal-forest vegetation.

Photo 9. Sinkhole and sawgrass at Lukens Creek.

Vegetation-Canopy DSM

A vegetation-canopy DSM was derived from a maximum-intercept DSM and the bare-earth DSM to obtain a surface model of canopy height in two steps. The results of a 2-m HPF in marsh zones and a 5-m HPF in forested zones were interpolated to a 2-m grid to derive a surface model of maximum-intercept values. Next, the bare-earth DSM was subtracted from the maximum-intercept DSM to obtain a surface model of vegetation-canopy heights, as normally observed from ground level.

Figures 9 - 11 show color-coded vegetation-canopy DSM. The boundary between the tidal marsh and the coastal forest is demarcated at canopy heights of ~1.4 m. Tall marsh types near this canopy height include black needlerush and sawgrass (Photo 10) and correspond to estimates of tidal-marsh canopy height made by Clewell (1997). Tall trees in hydric hammock exceeded 18 m in height (Photo 11). At Lukens Creek, considerable coastal-forest canopy is less than 7 m in height. This includes palmetto scrub, oak scrub, and scrubby flatwood on the sand hills (Photo 12). Data acquisition during August, with full-leaf cover, facilitated the extraction of the canopy-surface model from laser altimetry. Canopy-height characteristics can be obtained during summer when trees are fully leafed. However, winter-data acquisition would be preferable for a bare-earth model.

Photo 10. Thick sawgrass along a tidal-creek tributary to Waccasassa River.

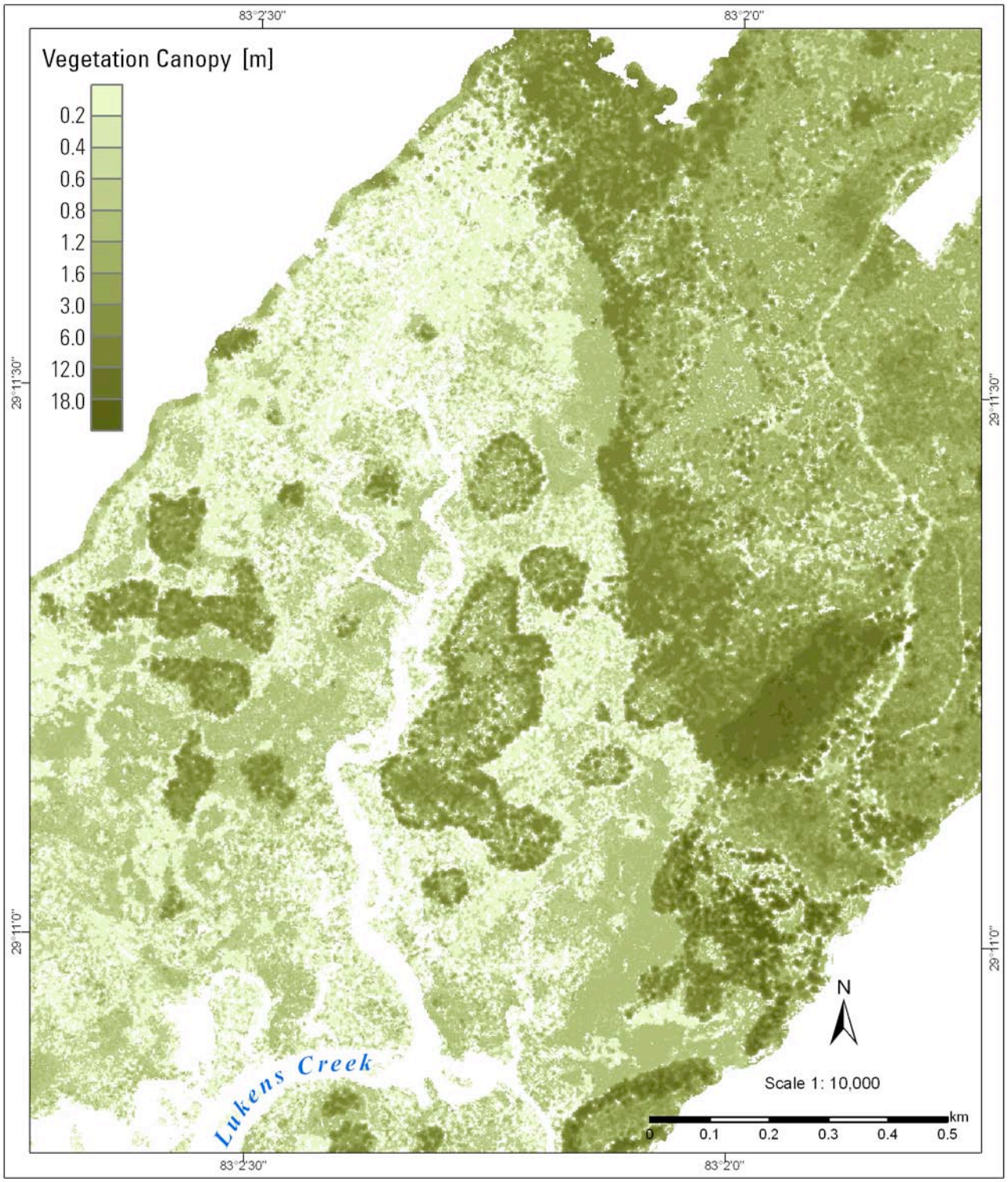

Figure 9. Canopy-height digital-surface model at Lukens Creek derived from ALSM.

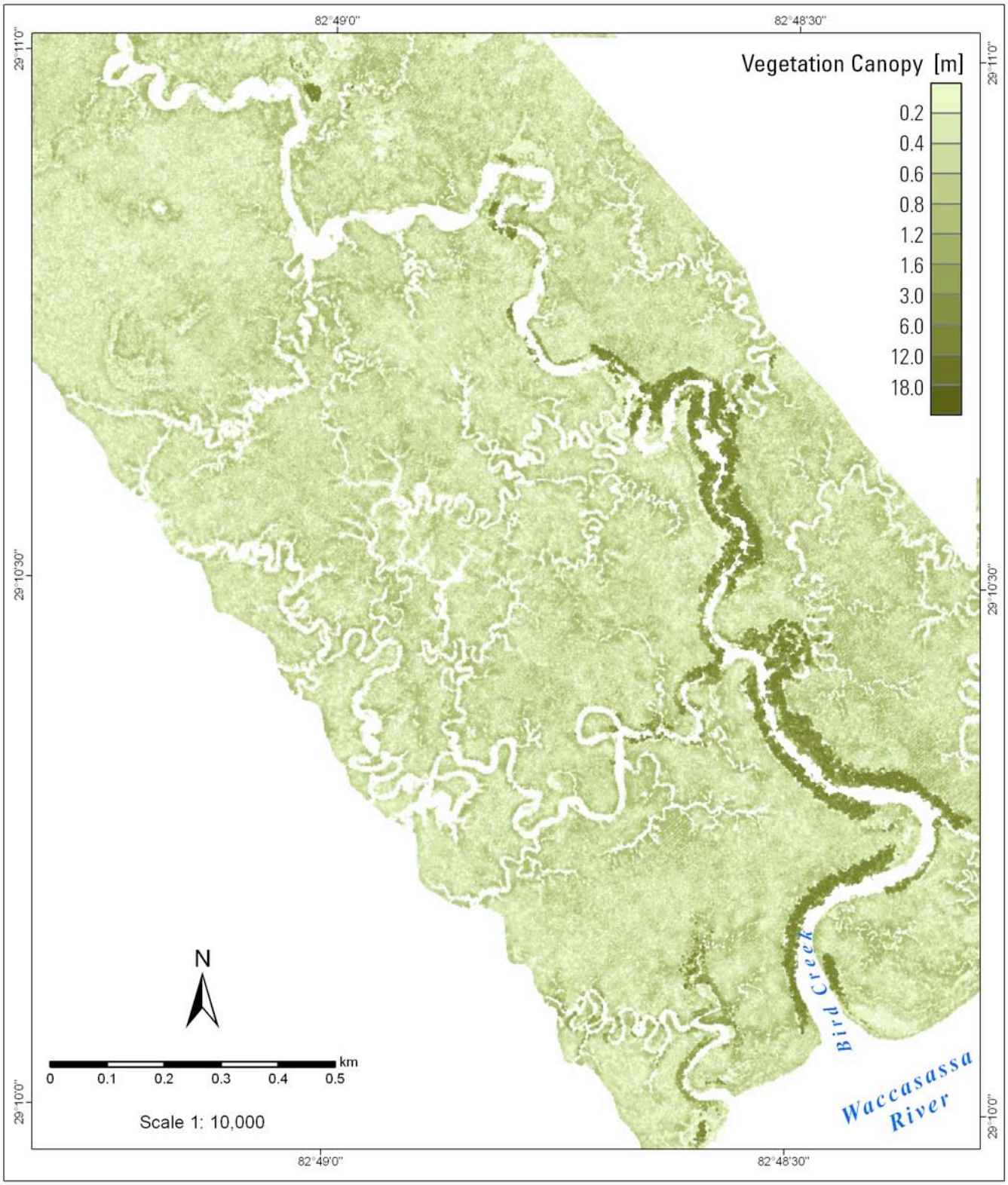

Figure 10. Canopy-height digital-surface model at Bird Creek derived from ALSM.

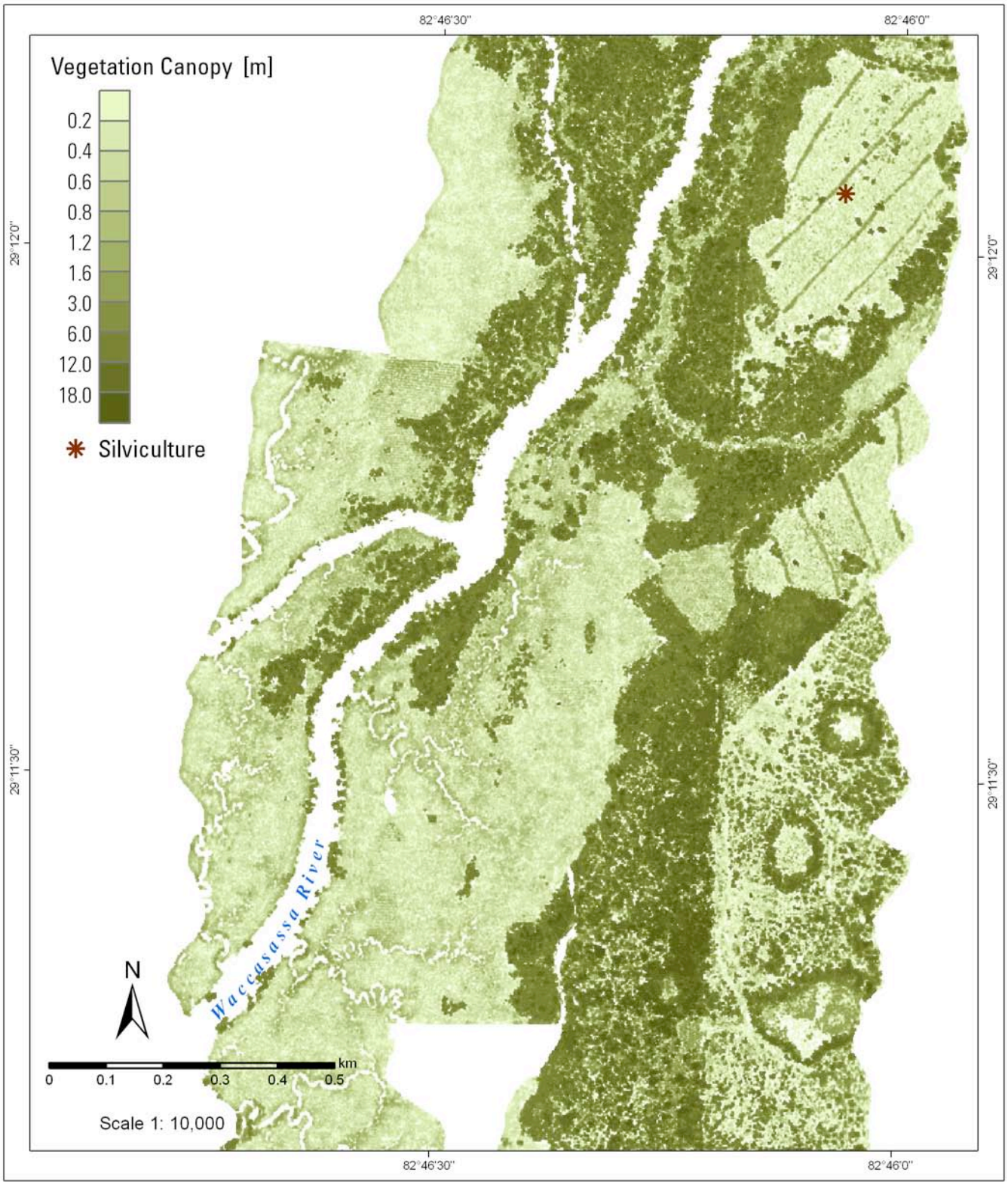

Figure 11. Canopy-height digital-surface model at Waccasassa River derived from ALSM.

Photo 11. Tall, thick-canopied hydric hammock in summer.

Photo 12. Open-canopy oak and palmetto scrub in sand hills.

Land-Cover Maps

Preliminary habitat maps were created from unsupervised classifications of bare-earth and canopy-height surface models and intensity values. The land-cover and habitat categories were selected to correspond with management programs for Cedar Key Scrub Reserve and Waccasassa Bay State Preserve (FDEP, 2005). An unsupervised classification was conducted using the bare-earth DSM, canopy-height DSM, and intensity values from the laser-altimetry dataset. Preliminary maps were created for each area (Figs. 12 - 14). Categories were validated through field reconnaissance, comparison with existing maps, and aerial photography. Categories for tidal marsh at four different flooding zones correspond to the single management category of estuarine tidal marsh. Sawgrass or depression wetlands occur in low-elevation swales between sand hills. Categories of sand-hill oak scrub and palmetto scrub were added to mesic and scrubby-flatwood categories to delineate distinct elevation and canopy-cover differences at high points on the sand hills and the low palmetto cover in open areas. Hydric hammock and mesic flatwood were more difficult to separate due to similarities in canopy height and canopy composition. Canopy height plays a greater role in this type of classification. Thus, differences between old-growth stands and fire-management recovery may be monitored (Photo 13). Burn areas in the marsh at Lukens Creek, sinkholes, limestone highs, silviculture, roads (Photo 14), and trails (Photo 15) can be seen in this map product.

Photo 13. Recovery of sand-hill oak scrub following fire management.

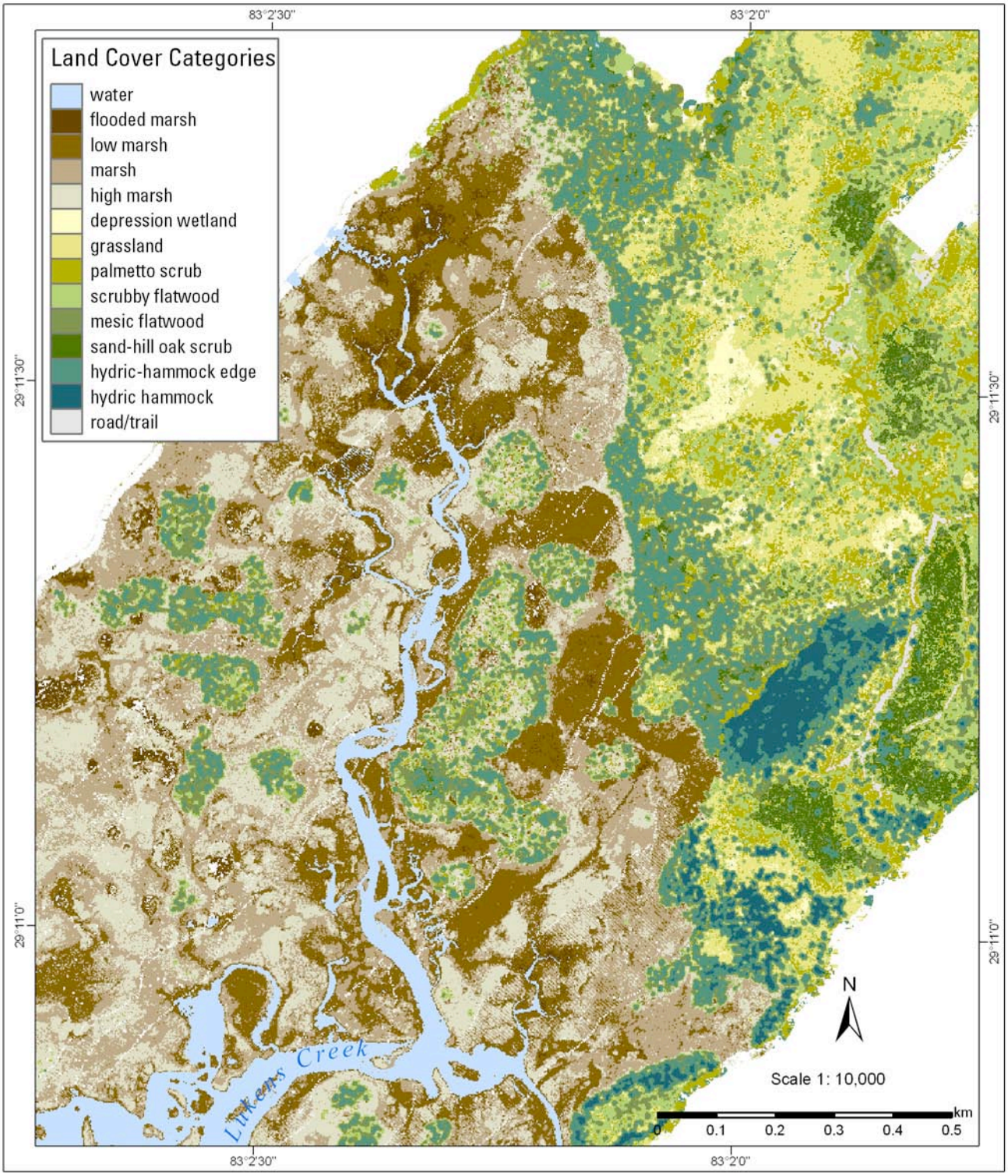

Figure 12. Lukens Creek land-cover categories derived from ALSM.

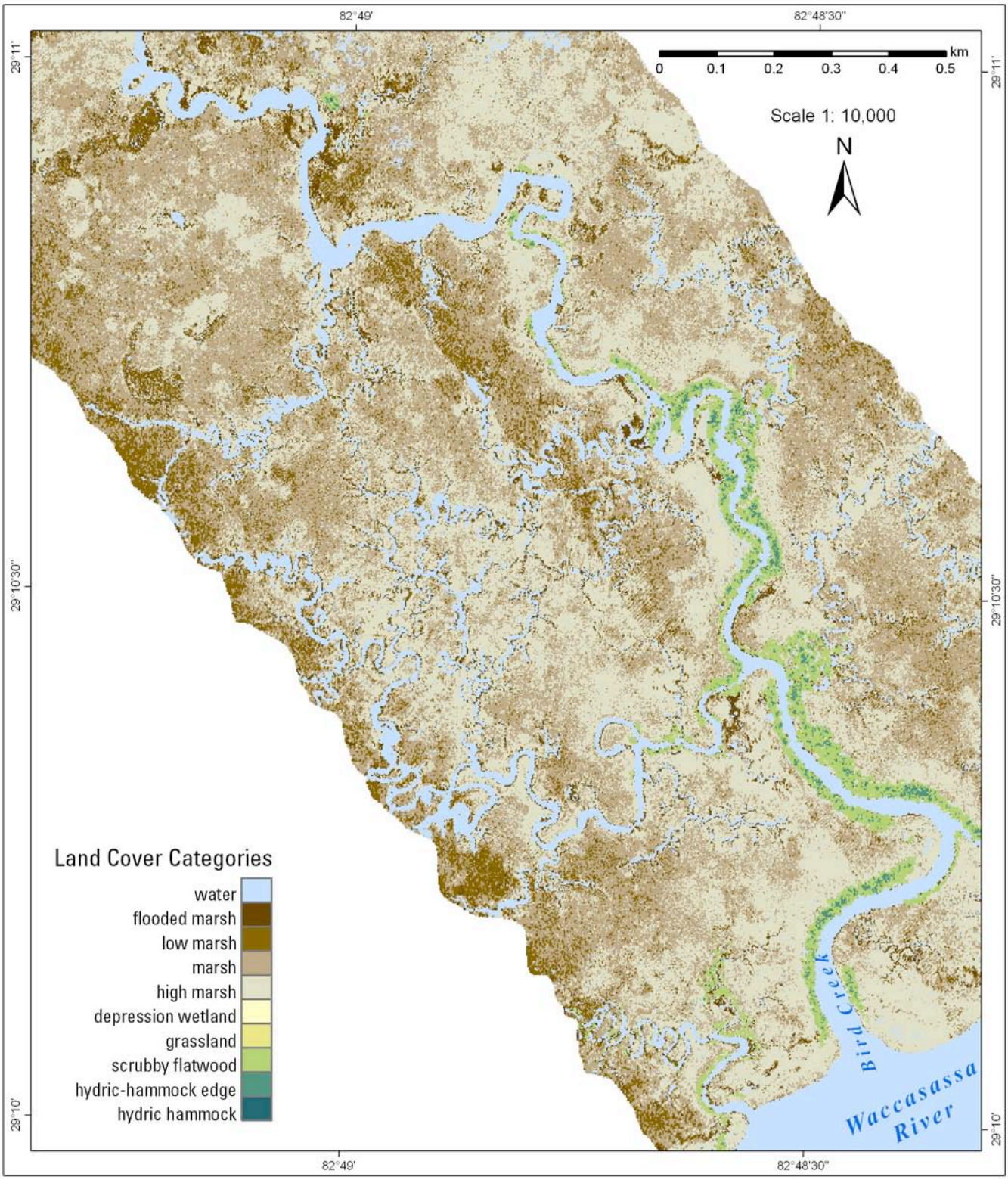

Figure 13. Bird Creek land-cover categories derived from ALSM.

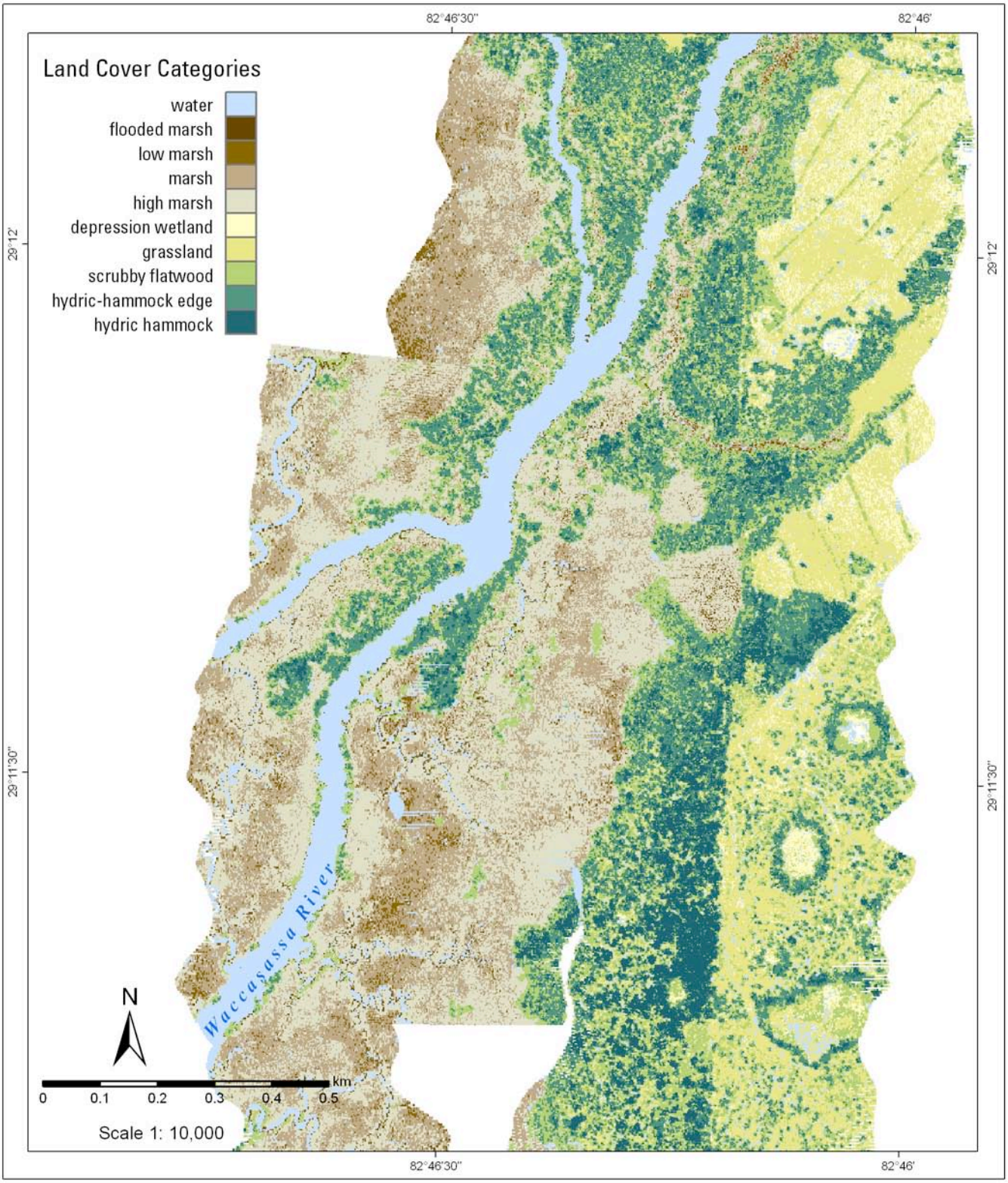

Figure 14. Waccasassa River land-cover categories derived from ALSM.

Photo 14. Scrubby flatwood along open sand road at Trail 8.

Photo 15. Game trails in high marsh at Lukens Creek.

Shoreline

Detailed shorelines were also extracted from the bare-earth DSM at the 0.2-m contour. This shoreline is more comprehensive than existing digital shoreline as shown in Figure 15 (FGDL, 2008; USGS, 2008). In an environment susceptible to flooding, storm impact, and sea-level rise, the morphology of tidal-creek drainages and changes over time are critical.

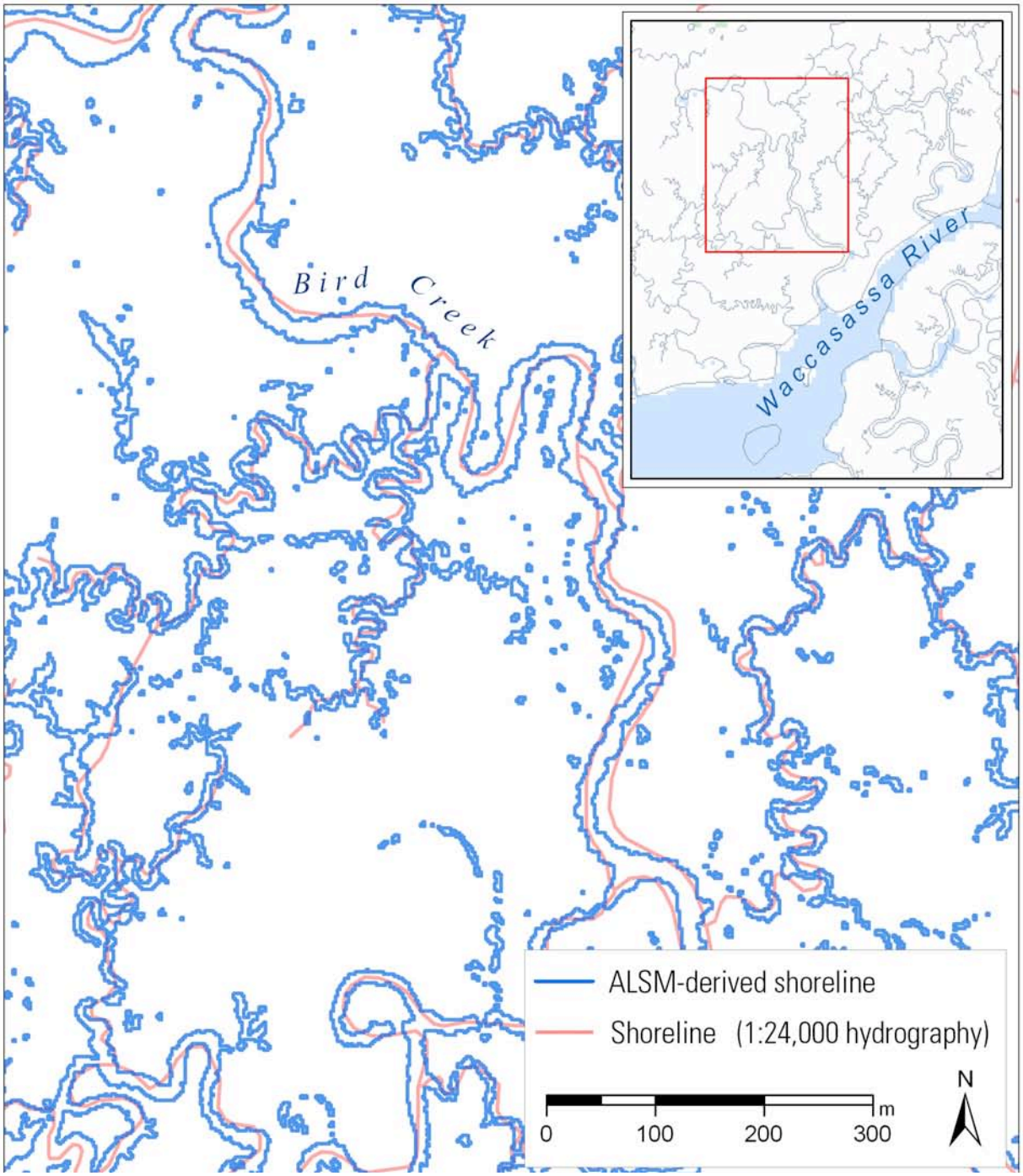

Figure 15. ALSM-derived shoreline compared to 1:24,000 hydrography (USGS) shoreline at Bird Creek.

Topographic-Profile Transects

Topographic profiles across bare-earth and canopy DSM were prepared as illustrations of marsh and coastal-forest geomorphology. Transects A-A1, B-B1, and C-C1 are located at Lukens Creek (Fig. 6). Transect D-D1 is located at Bird Creek (Fig. 7). Elevation point data for each transect were extracted from ground- and canopy-surface models and filtered with a 6-m-centered moving average (Figs. 16-19). The vertical axis is exaggerated (VE) in each profile to highlight subtle topographic relief. Notable characteristics are indicated by red arrows on Figures 16-19 and are listed below.

- Water level is depicted at 0.3 m for illustration purposes.
- Tidal-marsh elevations range from 0.3 to 0.9 m MSL and are marked for reference.
- The upper-elevation range of the tidal marsh, ~0.06 – 0.09 m, represents a transition from marine to terrestrial influence. Elevations below 0.9 m in the coastal-forest canopy indicate areas susceptible to flooding from both tidal and freshwater-surface flow.
- Lukens Creek has distinct tidal-creek levees (Fig. 16), but they are considerably lower than levees on Bird Creek (Fig. 19).
- Relict sand dunes are locally important, supporting an endemic oak-scrub habitat and associated faunal species (Figs. 16, 18).
- Sinkholes (circular features by air) appear as water-filled depressions in the transects (Figs. 16, 17).
- Forest remnants within the marsh: usually salt scrub and living or dead trees (Figs. 17, 18; Photos 7, 15).
- The absence of clearly defined surface drainage is characteristic of areas with thin sediment and near-surface limestone (Fig. 17).
- Where the transect crosses an historic shoreline or forest boundary, the historic-feature zone is marked (all figures; Raabe et al., 2004).
- Notches just to the interior edge of tree stands occur in the landward forest stands. Forest remnants closer to the coast appear to be missing the feature.
- Recent headward erosion of tidal creek is highlighted by low topography at the marsh interior (Fig. 18). Loss of forest soils and slow-sedimentation processes create a temporary topographic low during marine transgression (Raabe et al., 2004; Raabe et al., 2007).

The profiles show variations between high- and low-marsh canopies, and different creek and shore-edge forms, such as sloping or steep banks. Two characteristics, a canopy height less than 1.5 m and an elevation range of 0.3 to 0.9 m MSL (NAVD88), are key parameters of the tidal marsh. Higher elevations in the marsh tend to be toward the gulf, along levees, and high-marsh inland.

The coastal-forest elevation in these profiles ranges from about 0.5 to 2.5 m MSL (NAVD88). Forest-canopy height near the tidal marsh does not exceed 9 m. Game trails (Photo 15) and feral-hog ruts are common along this coast. Regardless of whether the forest-edge notches are the result of animal activity, a geomorphic process, or both, the coastal forest is vulnerable to flooding at these low points. Such notches are missing in forest remnants close to the coast, although a relict notch may be indicated where the forest has already converted to tidal influence.

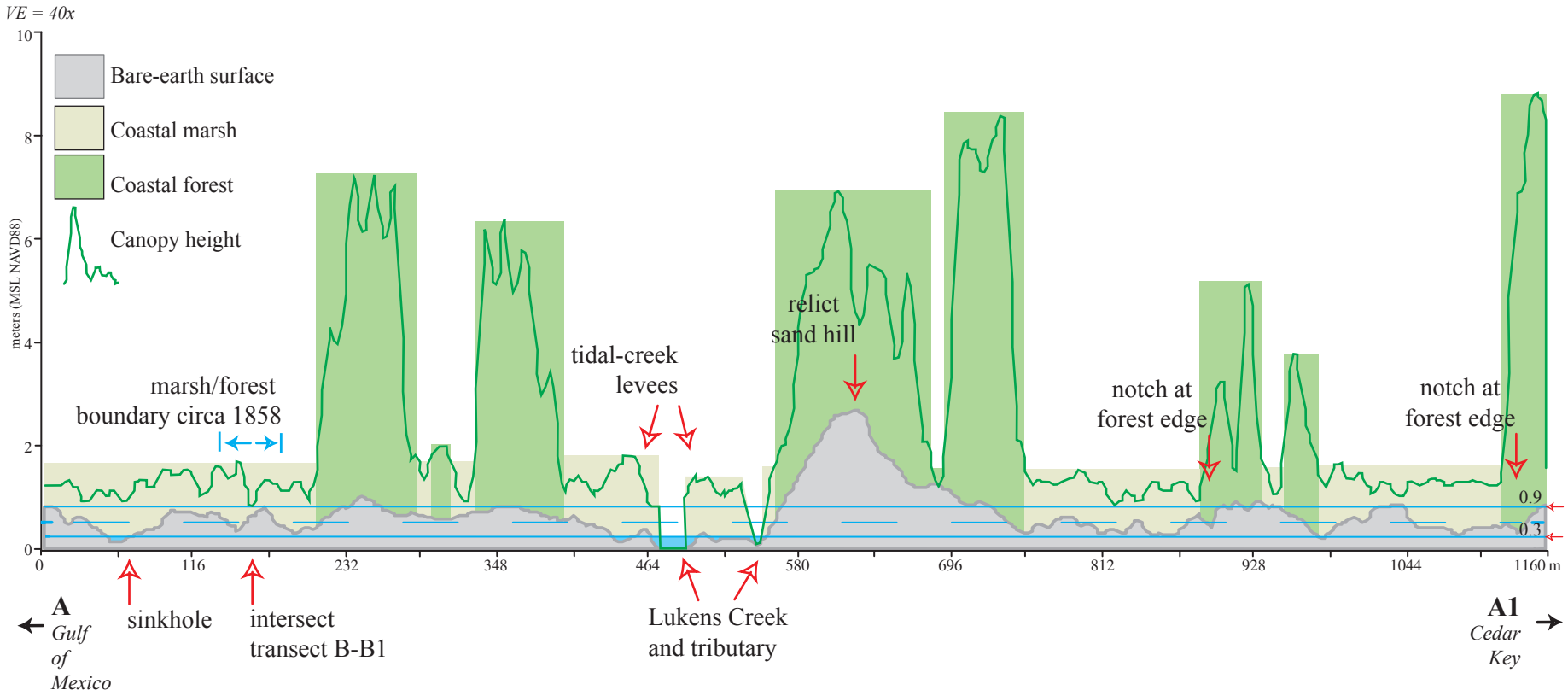

Figure 16. Transect A-A1 across Lukens Creek showing profile derived from bare-earth and canopy-surface models.

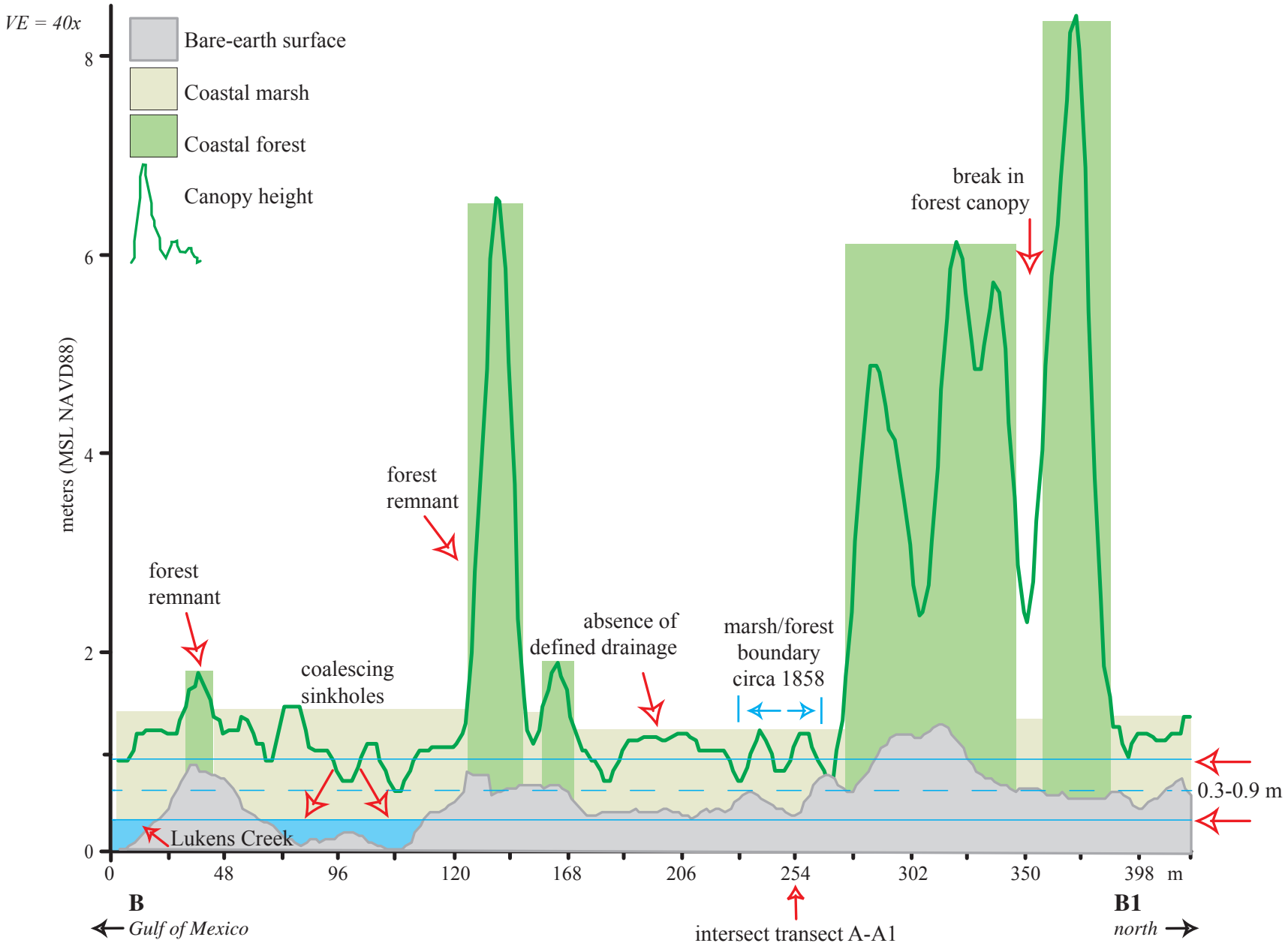

Figure 17. Transect B-B1 showing profile from Lukens Creek across tidal marsh and forest remnants.

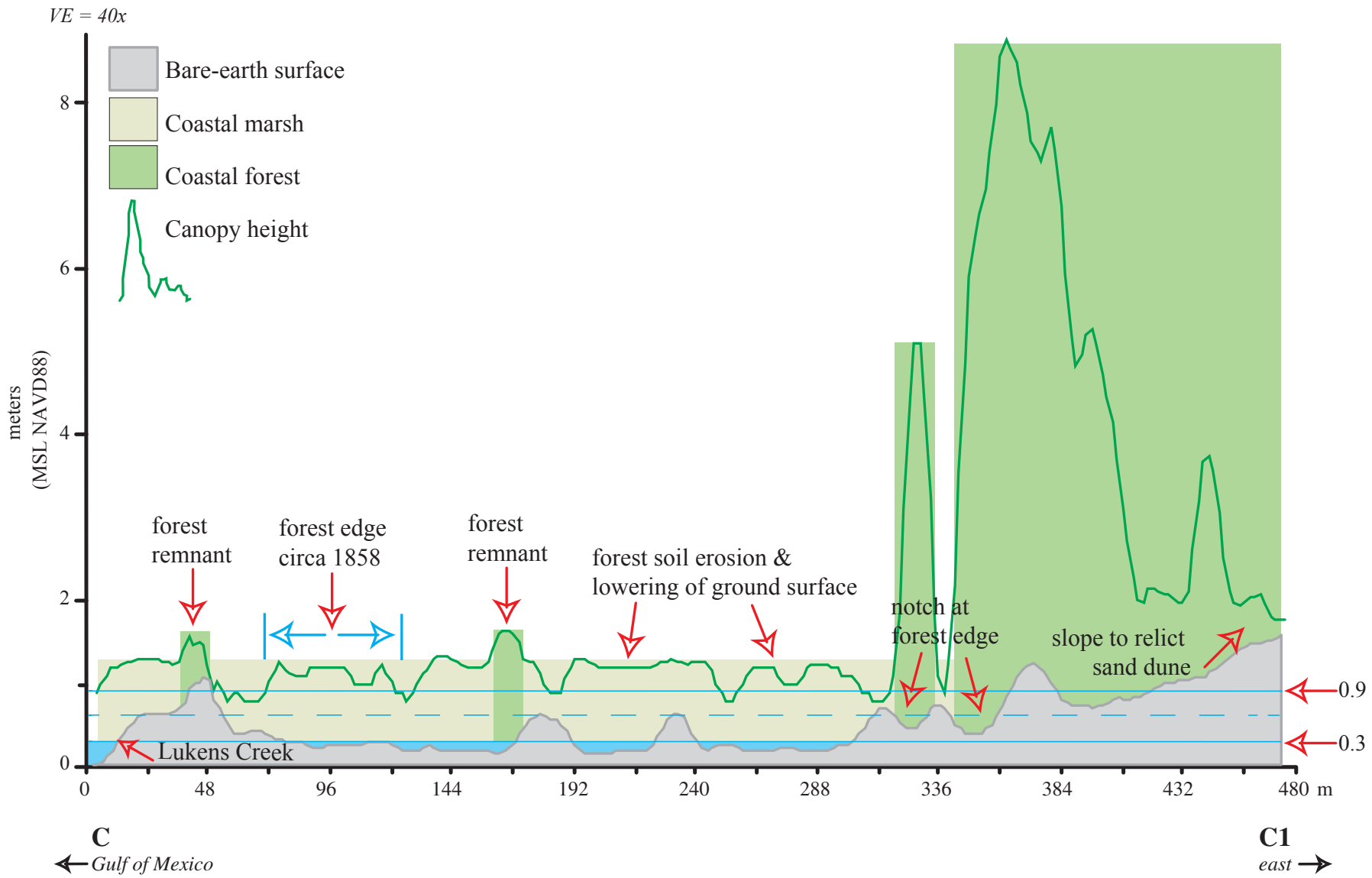

Figure 18. Transect C-C1 showing profile across upper reach of Lukens Creek to forest and relict dunes.

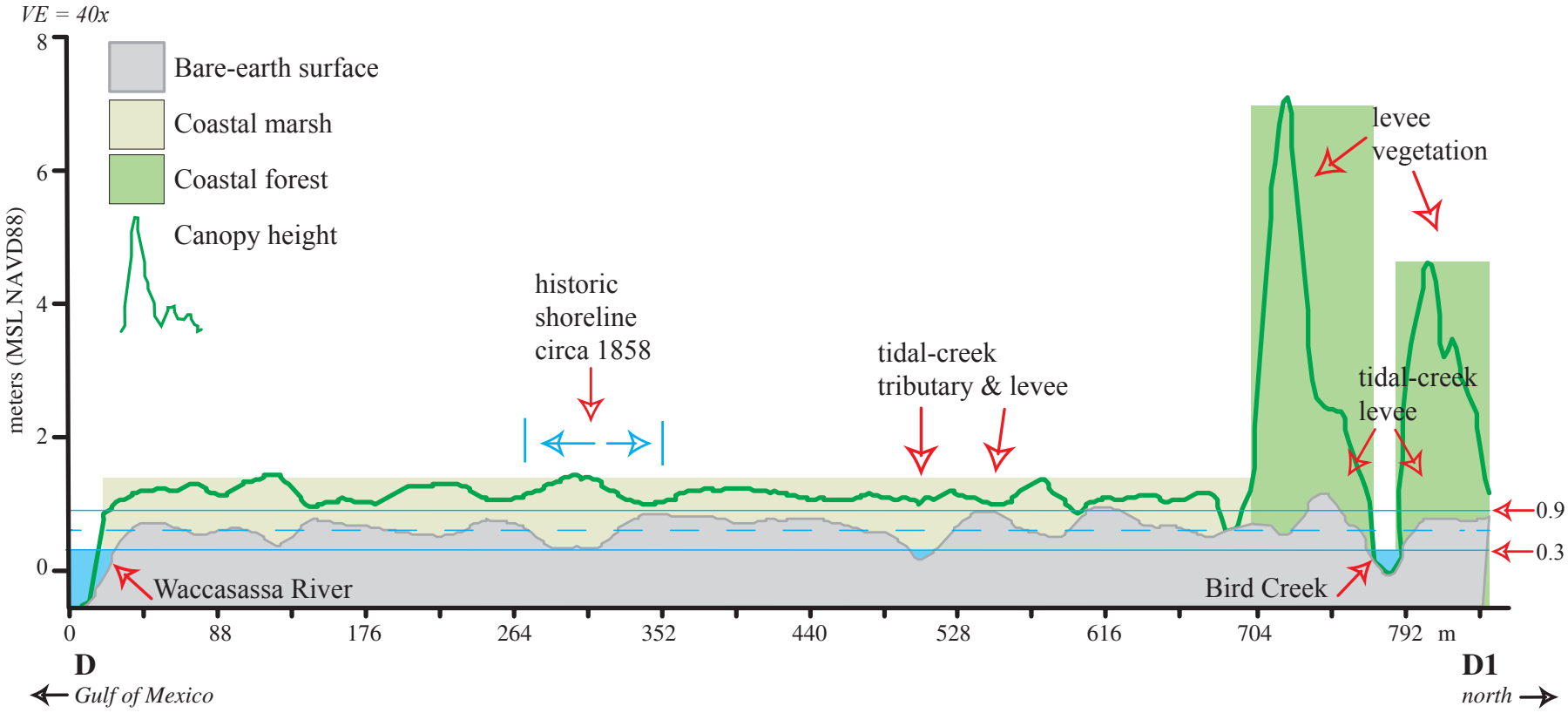

Figure 19. Transect D-D1 showing profile from Waccasassa River to a meander on Bird Creek.

Presence and absence of levees along tidal creeks can help distinguish areas with higher sediment supply. The Waccasassa River is situated at the head of an embayment that can serve to focus storm surge and suspended sediments at the river mouth. Higher river and creek levees near the mouth of the river could be attributed to sediment pulses focused in the embayment. This process may be exaggerated by logging activities in Gulf Hammock that have altered sediment supply and forest cover over the last 150 years (Raabe et al., 2004). The position of the historic shoreline at Bird Creek (Fig. 19) coincides with a topographic low. The apparent expansion of tidal marsh seaward may be attributable to the same process. Limestone control of the relatively deeper incised channels at Bird Creek and Waccasassa River also contributes to differing morphology from that at Lukens Creek.

Discussion

Previously unavailable topographic detail for this coastal environment was modeled successfully by sequential processing for three functionally unique landscape elements, using non-automated processing steps. The preservation of topographic features, such as tidal drainage, was feasible by partitioning the landscape into sections. Parameters for each feature were selected based on scale of feature, vegetation cover, and frequency of laser penetration to ground surface. Familiarity with local topography and landscape elements was key to modeling the surface in this way.

At Lukens Creek, the shorter canopy of the low marsh and the thin plant cover in burn areas provided consistent penetration of the laser and the extraction of ground intercepts with a 2-m LPF. However, the limited laser returns with this early instrument resulted in infrequent ground penetration in thick vegetation, particularly at Bird Creek and Waccasassa. A 10-m LPF was used to model the surface under thick forest canopy and marsh vegetation. Some micro-topographic features in the marsh are smoothed away with the use of a 10-m filter, but the final DSM adds considerable detail to existing digital-elevation models for the region.

Assessment of a DSM from field-survey O.H. is complicated by elevation variability across the area represented by a planar grid cell and the point represented by a field-surveyed O.H. We are confident that with new laser-altimeter instrumentation, multiple returns per pulse, and full-waveform systems (Brock et al., 2004; Lefsky et al., 1999), bare-earth models and canopy characteristics can be developed for coastal wetland and forested areas with ALSM.

The scale of features and processes may be deceptively small in a low-lying coastal system. Coastal wetlands are responsive to minor differences in the surface-drainage network, tidal flow, topography, and sediment supply. Currently available topography shows little or no geomorphic detail for this low-lying coastal zone and is too coarse to depict morphology where vertical difference between adjacent features is less than 0.5 m.

Laser-altimetry data were used to derive surface elevations for three areas of the coastal marsh in Levy County, Florida, where a combination of sediment deposition and erosion, limestone control, and human activities have helped to shape the coast. Processing of the ALSM data resulted in ground-surface models, detailed delineation of tidal-drainage patterns, vegetation-canopy heights, and preliminary land-cover maps. Topographic profiles extracted from both the bare-earth and canopy-height DSMs, show details of the coastal landscape. The geomorphic characteristics are important to understanding the evolution, stability, and vulnerability of this coastal system. Management efforts, such as control burn and recovery monitoring, can be enhanced with subsequent data acquisition. The results demonstrate the use of airborne laser-altimetry data to model the ground surface beneath vegetated coastal marsh and forest. The results further demonstrate the capacity to derive additional vegetative and geomorphic characteristics from ALSM data.

Acknowledgments

Jeffery DiMaggio, manager at Cedar Key Scrub Preserve, provided invaluable field assistance and expert knowledge. Elzbieta Bialkowska-Jelinska provided editorial and mapping support. Michael Sartori, a graduate student with University of Florida Civil Engineering Department, provided technical support.

References Cited

Ackerman, F., 1999, Airborne laser scanning - present status and future expectations: ISPRS Journal of Photogrammetry and Remote Sensing, v. 54, no. 2-3, p. 64-67.

Axelsson, P., 1999, Processing of laser scanner data - algorithms and applications: ISPRS Journal of Photogrammetry and Remote Sensing, v. 54, no. 2-3, p. 138-147.

Baltsavias, E.P., 1999, A comparison between photogrammetry and laser scanning: ISPRS Journal of Photogrammetry and Remote Sensing, v. 54, no. 2-3, p. 83-94.

Blair, J.B., Rabine, D.L., and Hofton, M.A., 1999, The Laser Vegetation Imaging Sensor: a medium-altitude, digitization-only, airborne laser altimeter for mapping vegetation and topography: ISPRS Journal of Photogrammetry and Remote Sensing, v. 54, no. 2-3, p. 115-122.

Brock, J.C., Wright, C.W., Clayton, T.D., and Nayegandhi, A., 2004, LIDAR optical rugosity of coral reefs in Biscayne National Park, Florida: Coral Reefs, v. 23, no. 1, p. 48-59.

Carter, W.E., Shrestha, R.L., and Thompson, P.Y., 1999, Airborne laser swath mapping of a portion of the Waccasassa marsh: University of Florida Department of Civil Engineering, Final Report submitted to the USGS, 18 p.

Clewell, A.F., 1997, Vegetation – Chapter 4, *in* Coultas, C.L. and Hsieh, Y.P., (eds.), Ecology and Management of Tidal Marshes, Delray Beach, FL, St. Lucie Press, p. 77-110.

Day, J.W., Scarton, F., Rismondo, A., and Are, D., 1998, Rapid deterioration of a salt marsh in Venice Lagoon, Italy: Journal of Coastal Research, v. 14, no. 2, p. 583-590.

Florida Department of Environmental Protection (FDEP), 2005, Waccasassa Bay Preserve State Park Unit Management Plan, Florida DEP: Division of Recreation and Parks, Division of State Lands, Tallahassee, FL, 150 p.

Florida Geographic Data Library (FGDL), 2008, USGS 1:24,000 Hydrography - Lines, *ftp://ftp1.fgdl.org/pub/county/levy/levy_core/.*

Fowler, R.A., Samberg, A., Flood, M.J., and Greaves, T.J., 2001, Topographic Lidar, *in* Maune, D.F., (ed.), Digital Elevation Model Technologies and Applications: The DEM Users Manual, ASPRS, p. 207-236.

Gomes Pereira, L.M., and R.J. Wicherson, 1999, Suitability of laser data for deriving geographical information: a case study in the context of management of fluvial zones: ISPRS Journal of Photogrammetry and Remote Sensing, v. 54, p. 105-114.

Hine, A.C., Belknap, D.F., Hutton, J.G., Osking, E.B., and Evans, M.W., 1988, Recent geologic history and modern sedimentary processes along an incipient, low-energy, epicontinental-sea coastline: Northwest Florida: Journal of Sedimentary Petrology, v. 58, no. 4, p. 567-579.

Iavarone, A., 2002, Laser Scanner Fundamentals: Professional Surveyor Magazine, v. 22, no. 9, *http://www.profsurv.com/archive.php?issue=68&article=949.*

Kraus, K., and Pfeifer, N., 1998, Determination of terrain models in wooded areas with airborne laser scanner data: ISPRS Journal of Photogrammetry and Remote Sensing, v. 53, no. 4, p. 193-203.

Lee, K.H., and Lunetta, R.S., 1995, Wetlands detection methods – Chapter 18, *in* Lyon, J.G. and McCarthy, J., (eds.), Wetland and Environmental Applications of GIS: Boca Raton, FL, CRC Press, Inc., p. 249-280.

Lefsky, M.A. Cohen, W.B., Acker, S.A., Parker, G.G., Spies, T.A., and Harding, D., 1999, Lidar remote sensing of the canopy structure and biophysical properties of Douglas-fir western hemlock forests: Remote Sensing of Environment, v. 70, no. 3. p. 339-361.

Lyon, J.G. and McCarthy, J., 1995, Introduction to wetland and environmental applications of GIS – Chapter 1, *in* Lyon, J.G. and McCarthy, J., (eds.), Wetland and Environmental Applications of GIS: Boca Raton, FL, CRC Press, Inc., p. 3-8.

Means, J.E., Acker, S.A., Fitt, B.J., Renslow, M., Emmerson, L., and Hendrix, C.J., 2000, Predicting forest stand characteristics with airborne scanning lidar: Photogrammetric Engineering and Remote Sensing, v. 66, no. 11, p. 1367-1371.

Mitsch, W.J., and Gosselink, J.G., 2000, Wetlands (3rd ed.): John Wiley & Sons, Inc., New York, 920 p.

Montague, C.L., and Odum, H.T., 1997, Setting and functions - Chapter 1, *in* Coultas, C.L., and Hsieh, Y-P., (eds.), Ecology and Management of Tidal Marshes: Delray Beach, FL, St. Lucie Press, p. 9-33.

Raabe, E.A., Stumpf, R.P., Marth, N.J., and Shrestha, R.L., 1996, A precise vertical network, establishing new orthometric heights with static surveys in Florida tidal marshes: Surveying and Land Information Systems, v. 56, no. 4, p. 200-211.

Raabe, E.A., and Stumpf, R.P., 1997, Assessment of acreage and vegetation change in Florida's Big Bend tidal wetlands using satellite imagery: Proceedings of the Fourth International Conference on Remote Sensing for Marine and Coastal Environments: Technology and Applications, 17-19 March 1997, Orlando, FL, p. 84-93.

Raabe, E.A., Marth, N.J., and Stumpf, R.P., 2000, GPS surveying of estuarine sites and water level gauges in the Lower Suwannee River watershed: U.S. Geological Survey Open-File Report 2000-296, 17 p.

Raabe, E.A., Streck, A.E., and Stumpf, R.P., 2004, Historic topographic sheets to satellite imagery: a methodology for evaluating coastal change in Florida's Big Bend tidal marsh: U.S. Geological Survey Open-File Report 2002-211, 44 p.

Raabe, E.A., and Bialkowska-Jelinska, E., 2007, Temperature anomalies in the Lower Suwannee River and tidal creeks: U.S. Geological Survey Open-File Report 2007-1311, 28 p. *(http://pubs.usgs.gov/of/2007/1311/)*.

Raabe, E.A., Edwards, R.E., McIvor, C.C., Grubbs, J.W., and Dennis, G.D., 2007: Habitat and Hydrology: Assessing Biological Resources of the Suwannee River Estuarine System: U.S. Geological Survey Open-File Report 2007-1382 (*http://pubs.usgs.gov/of/2007/1382/*).

Rupert, F.R., and Arthur, J.D., 1997, Geology and geomorphology - Chapter 2, *in* Coultas, C.L., and Hsieh, Y-P., (eds.), Ecology and Management of Tidal Marshes: Delray Beach, FL, St. Lucie Press, p. 35-52.

Sallenger, A.H., Krabill, W.B., Swift, R.N., Brock, J., List, J., Hansen, M., Holman, R.A., Manizade, S., Sontag, J., Meredith, A., Morgan, K., Yunkel, J.K., Frederick, E., and Stockdon, H., 2003, Evaluation of airborne topographic Lidar for quantifying beach changes: Journal of Coastal Research, v. 19, no. 1, p. 125-133.

Shrestha, R.L., Carter, W.E., Lee, M., Finer, P., and Sartori, M., 1999, Airborne laser swath mapping: accuracy assessment for surveying and mapping applications: Surveying and Land Information Systems, v. 59, no. 2, p. 83-94.

Stoddard, D.R., Reed, D.J., and French, J.R., 1989, Understanding salt-marsh accretion, Scolt Head Island, Norfolk, England: Estuaries, v. 12, no. 4, p. 228-236.

Stumpf, R.P., and Haines, J.W., 1998, Variation in tidal level in the Gulf of Mexico and implications for tidal wetlands: Estuarine and Coastal Shelf Science, v. 46, no. 2, p. 165-173.

USGS, 2007, U.S. Geological Survey National Elevation Data Set, *http://ned.usgs.gov/*.

USGS, 2008, U.S. National Hydrography Dataset, *http://edc2.usgs.gov/geodata/index.php*

Vernon, R.O., 1951, Geology of Citrus and Levy Counties, Florida: Florida Geological Survey Bulletin, no. 33, 256 p.

Vosselman, G., 2000, Slope based filtering of laser altimetry data: International Archives of Photogrammetry and Remote Sensing, v. 33, p. 935- 942.

Williams, K., Ewel, K.C., Stumpf, R.P., Putz, F.E., and Workman, T.W., 1999, Sea-level rise and coastal forest retreat on the west coast of Florida, USA: Ecology, v. 80, no. 6, p. 2045-2063.

Appendix I

Table 3. Orthometric heights (O.H.) of ground control points (GCP) and base stations.

GCP#	Eastings	Northings	O.H. (m) MSL NAVD88	Re-occupy[1] O.H. (m)	Description	Plant height (m), if given
Base 1	302055.826	3231090.068	0.531	0.531/0.498	rebar	
1	302031.132	3231096.593	0.452		sawgrass	1.1
2	302022.295	3231103.066	0.448		*Juncus*	0.9
3	302018.445	3231116.658	0.449		*Distichlis*	0.3
4	302013.666	3231127.162	0.446		*S. alterniflora*	0.2
5	302011.809	3231132.294	0.436		sawgrass	1.1
6	302010.656	3231138.745	0.442		sawgrass	1.1
7	302008.626	3231145.099	0.436		*Juncus*	1.2
8	301999.216	3231146.593	0.441		*Juncus*	1.0
9	301991.783	3231144.283	0.447		*Juncus*	1.1
10	301986.098	3231141.831	0.444		*Batis maritima*	0.2
11	301976.551	3231135.456	0.549	0.562	*Borrichia/B. maritima*	0.2
12	301971.283	3231134.549	0.615		*Batis maritima*	0.1
13	301969.698	3231132.914	0.654		*J. coriaceae*	0.5
14	301968.322	3231126.508	0.746		*Iva/Baccharus* salt scrub	1.4
15	301965.411	3231115.693	0.739		*Iva/Baccharus* salt scrub and Sabal	1.4
16	301953.474	3231117.342	0.516		*Batis maritima*	0.2
17	301950.712	3231154.419	0.459		*Distichlis/B. maritima*	0.3
18	301956.363	3231171.726	0.462		*S. alterniflora*	0.2
19	301952.754	3231187.975	0.433		*Distichlis*	0.4
20	301941.592	3231211.894	0.435		*Distichlis/B. maritima*	0.3
21	301937.022	3231228.825	0.443		*Batis maritima/Distichlis*	0.3
22	301932.097	3231242.103	0.469	0.470	Dead Sabal/*B. maritima/S. alterniflora*	0.3
23	301929.396	3231249.024	0.447		*S. alterniflora*	0.2
24	301916.816	3231275.295	0.359		*S. alterniflora* flooded	0.2
25	301909.965	3231289.716	0.344		*S. alterniflora* flooded	0.4
26	301888.210	3231319.805	0.385		*S. alterniflora* flooded	0.3
27	301877.378	3231334.627	0.399		*S. alterniflora* flooded	0.4
28	301872.716	3231346.238	0.399		Distichlis	0.3
29	301862.988	3231363.037	0.392		*Juncus*	1.5
30	301847.966	3231377.488	0.346		*S. alterniflora*	0.3
31	301822.329	3231396.891	0.419		*Distichlis*	0.3

32	301873.255	3231422.171	0.404		*S. alterniflora/Juncus*	1.1
33	301878.926	3231418.193	0.894		Dead Sabal trunk; root base 0.6 m above surrounding ground surface	6.0
34	301905.180	3231411.972	0.466		*Distichlis*	0.3
35	301939.941	3231447.511	0.551		Forest edge/transition with *Distichlis*	0.3
36	301937.492	3231446.555	0.554	0.537	Forest edge/transition with dry *Distichlis*	0.3
37	302073.243	3231099.418	0.285		Sawgrass edge	
38	302080.383	3231103.660	0.488		High marsh mix	
39	302085.899	3231106.574	0.549		Palmetto	
40	302086.827	3231107.441	0.819		50% Canopy mixed wood	
41	302098.045	3231113.550	0.846		Pine mixed forest	
42	302129.326	3231131.164	1.302		Thick oak and mix canopy	
43	302159.966	3231148.283	1.654		Thick scrub oak	
44	302061.522	3231093.215	0.457		*Juncus* marsh	
45	302068.842	3231097.356	0.482		*Juncus* marsh	
46	302076.347	3231101.123	0.478		*Juncus* marsh	
47	302084.951	3231105.621	0.532		Open palmetto and pine	
48	302092.682	3231111.146	0.842		Hydric hammock mixed	
49	302100.925	3231114.804	0.862		Pine/palmetto	
50	302108.784	3231118.941	0.997		Pine scrub	
51	302116.453	3231124.144	1.208		Palmetto oak scrub	
52	302124.847	3231128.864	1.193		Pine and oak scrub	
53	302133.589	3231133.741	1.375		Palmetto oak scrub	
54	302142.147	3231138.495	1.509		Oak scrub	
55	302149.817	3231142.728	1.580		Oak palmetto scrub	
56	302157.447	3231147.133	1.700		Thick scrub oak	
57	302162.512	3231149.897	1.701		Thick scrub oak	
Base 2	324093.641	3227528.102	0.861	0.861/0.861	*Juncus/S. alterniflora* boundary - base station on Lone Cedar Island	
58	324310.805	3228342.773	0.736	0.736	levee: *Juncus/Distichlis*	
59	324312.117	3228329.977	0.593		levee: *Juncus* boundary	
60	324313.852	3228315.391	0.494		wrack barren	
61	323951.578	3229001.766	0.542		wrack barren	
62	323965.188	3229001.234	0.501		*Juncus* clump	
63	323970.203	3229003.328	0.612		*Distichlis* at tree edge	
64	323708.531	3229160.438	0.493	0.496	levee: *Juncus* edge	
65	323711.906	3229160.078	0.566		levee: *Iva*/sedge	
66	323714.234	3229163.352	0.493		levee edge: *S. patens/Juncus*	
66	323720.836	3229167.977	0.373		thick *Juncus*	

67	323262.781	3229394.141	0.363	0.362	*Juncus*	
68	323257.805	3229394.195	0.341		wetter *Juncus*	
69	323253.625	3229394.648	0.322		wetter *Juncus*	
70	323105.828	3229964.828	0.252		*Juncus*	
71	323107.891	3229950.461	0.247		*Juncus*	
72	327205.930	3228549.805	0.322	0.325	wet *Juncus*	
73	327214.359	3228536.367	0.311		wet *Juncus* - last of drainage	
74	327229.508	3228503.094	0.447		short dry *Juncus* spp.	
75	327146.328	3228617.359	0.373		Sawgrass	
76	324176.688	3228436.555	0.581	0.582	levee edge - dry mud	
77	324180.648	3228443.438	0.792		levee hammock/mud boundary	
78	324189.445	3228450.383	0.761		levee hammock	
79	324196.430	3228471.992	0.549		back edge of levee hammock	
80	324200.617	3228475.984	0.574		high marsh salt scrub	
81	324210.672	3228482.125	0.536		*Juncus*	
82	324213.844	3228487.242	0.500		*Juncus*	
83	324094.654	3227542.190	0.629		*Distichlis/Juncus/Salicornia/Iva*/dead palm on Cedar Island.	
84	323992.809	3227752.155	0.791		Sabal/cedar/*Iva* no seedlings	
85	323997.911	3227767.596	0.868		Hammock interior/Sabal seedlings/Cedar/wrack	

[1]Repeat occupation of a ground control site or base station